TRIBHUVAN UNIVERSITY

INSTITUTE OF ENGINEERING

PULCHOWK CAMPUS

THESIS NO: M-74-MSMDE-2021-2023

EXPERIMENTAL CHARACTERIZATION AND AEROELASTIC ANALYSIS OF A COMPOSITE WING

by

ABHISHEK BHANDARI

A THESIS

SUBMITTED TO THE DEPARTMENT OF MECHANICAL AND AEROSPACE ENGINEERING IN PARTIAL FULFILLMENT OF THE REQUIREMENTS FOR THE DEGREE OF MASTERS OF SCIENCE IN MECHANICAL SYSTEM DESIGN AND ENGINEERING

DEPATRMENT OF MECHANICAL AND AEROSPACE ENGINEERING

LALITPUR, NEPAL

NOVEMBER, 2023

Copyright

TRIBHUVAN UNIVERSITY

INSTITIUTE OF ENGINEERING

PULCHOWK CAMPUS

DEPARTMENT OF MECHANICAL AND AEROSPACE ENGINEERING

The undersigned certify that they have read, and recommended to the Institute of Engineering for acceptance, a thesis entitled " **Experimental Characterization and Aeroelastic Analysis of a Composite Wing**" submitted by Abhishek Bhandari in partial fulfillment of the requirements for the degree of Master in Mechanical Systems Design and Engineering.

Prof. Dr. Laxman Poudel,
Department of Mechanical and Aerospace Engineering

Asst. Prof. Dr. Sudip Bhattarai,
Supervisor,
Department of Mechanical and Aerospace Engineering

Er. Ashish Manandhar,
External Examiner,
MPC Engineer, Himalaya Airlines Pvt. Ltd.

Prof. Dr. Laxman Poudel
Program Coordinator,
Department of Mechanical and Aerospace Engineering

Tribhuvan University
Institute of Engineering
Department of Mechanical and Aerospace Engineering
Pulchowk Campus

Committee Chairperson,
Asst. Prof. Dr. Sudip Bhattarai
HOD of Mechanical and Aerospace Engineering

Date: 26/11/2023

Abstract

A UAV's wing, which affects its flight dynamics and capability, is essential to its efficiency. Traditional materials have their advantages, but they frequently sacrifice strength or weight. Aircraft wing design must strike a balance between flight efficiency, structural soundness, material selection, and manufacturing constraints. Acknowledging this, considerations for necessary design factors such as flight requirements, selection of airfoil profile, wing loading, selection of material, weight considerations and standardized placement of reinforcing frame components are made. Focusing on strength, lightweight, and adaptability, composite materials, particularly fiberglass with polymers and the combination of balsa skeleton, have been used. Use of digital manufacturing technology and versatile materials like fiberglass and balsa allowed for controlling design parameters of the wing to obtain desired vibrational and structural properties while reducing weight. Finite element analysis, such as structural and modal analysis are used in conjunction to validate the structural properties of the wing. Following that experimental modal analysis was conducted, to obtain frequency of first mode of longitudinal vibration under different loading conditions, by processing motion capture data in MATLAB. The research has employed both numerical simulations and experimental analysis to design, construct and test the aeroelastic properties of the composite wing.

Acknowledgment

I would like to extend my sincere thanks and deep sense of gratitude to Prof. Dr. Laxman Poudel and Asst. Prof. Dr. Sudip Bhattarai, IOE, Pulchowk, for supervising my thesis work. I would also like to express my sincere thanks to my respected teachers in IOE, Pulchowk, namely: Prof. Dr. Mahesh Chandra Luintel, Asst. Prof. Kamal Darlami, and Asst. Prof. Ashish Karki for their valuable guidance. Constant support, motivation, and encouragement from them have been pivotal in carrying out the research works.

I am thankful to the Department of Mechanical and Aerospace Engineering for continuous technical guidance and for providing workspace and manufacturing facilities equipped with digital manufacturing capabilities and high-speed image capture setup. A special thanks to my friends, Er. Rajan Basnet, Er. Salim Maharjan, Er. Akin Chhetri, Er. Bibek Adhikari, Er. Sandip Gewali, Er. Anup Pandey, Prashant Sharma Prasar, Aniket Gupta, and Hemanta Neupane for their continuous motivation and support during hard times.

Lastly, I will always be in debt to my beloved family; my father, Mr. Pramod Bhandari, my mother, Mrs. Goma Devi Koirala, and my sister, Barsha Bhandari, for encouraging me to pursue my engineering dream and to give back to society with my resource, knowledge, and capability.

Table of Contents

List of Figures

List of Tables

List of Acronyms and Abbreviations

UAVs	Unmanned aerial vehicles
OPPA	One-Pitch Phase Analysis
TPU	Thermoplastic polyurethane
XFLR	Analysis tool for airfoils, wings and planes operating at low Re.
VLM	Vortex lattice method
FEA	Finite element analysis
PMCs	Polymer Matrix-based Composites
DIC	Digital Image Correlation
FDM	Fused Deposition Modeling
PLA	Polylactic Acid
CNC	Computer Numeric Control
FRF	Frequency Response Functions
GSM	Grams per square meter
DXF	Drawing Exchange Format
TIFF	Tag Image File Format
PSD	Power Spectral Density
AOA	Angle of Attack

CHAPTER ONE: INTRODUCTION

1.1 Background

In the rapidly evolving landscape of aviation, Unmanned Aerial Vehicles (UAVs) have established a niche for themselves, finding applications in diverse sectors such as military operations, aerial photography, surveying, agriculture, and even delivery services. Central to the functionality of a UAV is its wing, a component that plays a pivotal role in ensuring the UAV's flight stability, control, and efficiency.

This research delves into development and experimental characterization of a UAV wing that incorporates fiberglass composite skin and balsa skeleton. The wing design involves its initial considerations and selection of airfoil profile, area of the wing, wing loading characteristics, material, and weight of the wing (Mostakim et al,2019). The choice of materials is not arbitrary. As emphasized by Oladele et al (2020), the 21st century has witnessed the rise of polymers as a material par excellence, owing to their unparalleled properties. Fiberglass, a renowned fiber-reinforced polymer, emerges as an ideal candidate for wing design due to its commendable strength-to-weight ratio and durability. Balsa wood was selected for the wing frame structure, for its impressive weight-to-strength ratio. Its ease of use makes it ideal for quick design adjustments and rapid prototyping. The wood can also absorb and distribute stress aiding in its resilience. Further its natural vibration dampening properties also contribute to a smoother flight, reducing the impact of minor turbulence.

The journey of designing a UAV wing is full of challenges, demanding a balance between flight performance, structural integrity, material choice and cost considerations. This research explores the fabrication of a fiberglass skin through an advanced hand layup process followed by vacuum bagging, while the internal structure is made of a laser-cut balsa wood skeleton. The culmination of these components results in a UAV wing that promises durability and reliability. To validate the structural properties of the wing, finite element analysis is employed, complemented by an experimental motion capture setup to perform modal analysis. By incorporating advanced materials, modern design approach and manufacturing techniques, this research attempts to create a wing that is more durable, reliable, and efficient and to develop a suitable test method to evaluate its reliability.

1.2 Research Gap

The essence of a UAV's effectiveness lies in its wing, influencing its flight dynamics and capacity. The aviation world is rapidly evolving, with UAVs taking center stage in fields from defense to entertainment.

In the paper Mostakim et. el (2019), the authors have conducted modal analysis to ascertain the natural frequencies and mode shapes of the wing. This was done by employing software simulation followed by experiments utilizing an eddy current displacement sensor. The researchers observed comparable results for the 1st natural frequency, thereby validating their work. The authors opted for Balsa Wood as the material for the wing, complemented by a thin layer of sticker. To enhance structural performance and durability, a recommended modification involves substituting the thin sticker layer with a lightweight and robust fiberglass skin. This strategic change in skin material is employed in the current research to contribute to an overall improvement in the wing's mechanical properties and longevity.

The paper by Morimoto has explored applications of a real-time motion capture technique called OPPA (one-pitch phase analysis) by employing it for modal analysis of free vibration of a flat cantilever plate after hammering. Building upon this research, the current research employs visual tracking methods to perform modal analysis of a wing modelled as a cantilever beam.

While traditional materials have their merits, they often compromise on weight or strength. Composite materials, especially fiberglass with polymers, with the combination of balsa skeleton emerge as a promising alternative due to their strength, lightness, and adaptability. Using these materials in wing design is not simple. It demands a thorough grasp of their properties and design nuances. Further validating the choices made in the design process using structural analysis is a core part of this paper. This research dives into creating and testing a wing using fiberglass composite and balsa, aiming to develop a highly efficient and durable wing for long-range cruise UAV’s.

1.3 Objectives

The main objective of the research is to design a composite wing that utilizes versatile materials like balsa and fiberglass with considerations to the desired aerodynamic characteristics, weight, and load-bearing capabilities.

1.3.1 Specific objectives

- To fabricate the fiberglass composite skin, fabricate the skeleton structure and assemble the prototype using established standards and practices.
- To perform FEA analysis of the modelled wing structure.
- To build test rig suitable for structural testing of the prototype.
- To conduct experimental testing for modal analysis and aeroelastic analysis of the wing.

1.4 Limitations

- The study only considers first mode of longitudinal vibration for modal analysis and does not study consider the nature of higher modes of vibration. This decision was based on the review that first mode of longitudinal vibration is the most significant mode of vibration for a cantilever wing model experiencing lift load.
- For the current research removal of air from the vacuum bag was done by a manually operated pump. So, complete evacuation of air from the bag could not be ensured.
- An attempt in experimentation involving aerodynamic loading in open channel wind tunnel by varying actual aerodynamic loading conditions could not be completed.

CHAPTER TWO: LITERATURE REVIEW

2.1 Design and Modelling

The wing serves as a vital component of an aircraft, acting as a lifting surface when in motion through a fluid medium, typically air. A wing is classified as a fin and its design plays a critical role in the aircraft's performance. The effectiveness and efficiency of an aircraft are largely contingent upon the quality of the wing design. The design of a UAV wing requires a trade-off between flight performance, structural requirements, and cost. A thorough understanding of the flight requirements and the trade-offs between different design options is crucial in deciding the design of a UAV wing.

The value of lift force generated by a wing is calculated using the lift equation 2.1:

$$L = \frac{1}{2} \times C_l \times \rho \times A \times v^2 \quad (2.1)$$

Where, L is the lift force

ρ (rho) is the air density

v is the velocity of the air relative to the object

A is the reference area (typically the wing area for an aircraft)

C_l is the coefficient of lift, which depends on the shape of the object and its AOA.

Aeroelasticity deals with the interactions between aerodynamic forces and structural dynamics, and analyzing how these interactions affect the overall behavior of the wing. The two most dramatic aeroelastic effects are flutter and divergence. Flutter is a dynamic instability caused by positive feedback between wing deflection and aerodynamic lift and drag forces (Aerospace Engineering Blog, 2017). The airspeed at which the wing, or any other component of the structure, begins to vibrate with zero net damping and experiences simple harmonic motion, akin to the basic to and fro motion of a simple pendulum, is known as the flutter speed. Since there is no energy dissipation when there is zero net damping, any additional reduction in net damping would cause self-oscillation, where the structure is essentially causing itself to vibrate more and more, which eventually lead to failure.

For underdamped free vibrations, the system oscillates about an equilibrium position. However, the system's overall energy level decreases each time it enters equilibrium. With each cycle of motion, the maximum displacement is continuously decreasing. Figure (2.1) and Equation (2.2) demonstrate how the amplitude diminishes exponentially with time.

$$x(t) = Ae^{-\zeta\,\omega_n t}\sin(\omega_d t + \phi_d) \tag{2.2}$$

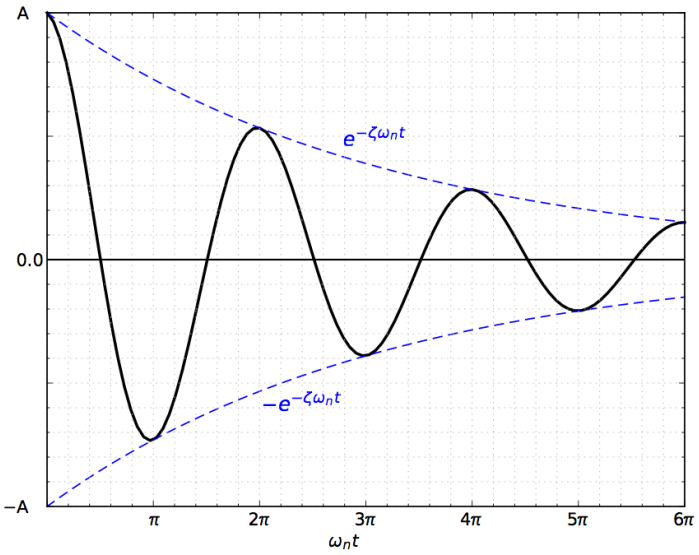

Figure 2.1: Free vibrations of an underdamped SDOF system decaying exponentially (A., Drang, 2014)

The logarithmic decrement, δ, is defined for underdamped free vibrations as the natural logarithm of the ratio of the amplitudes of vibration on successive cycles.

$$\delta = ln(\frac{x(t)}{x(t+T_d)}) \tag{2.3}$$

The logarithmic decrement is often measured by experiment and damping ratio determined from

$$\zeta = \frac{\delta}{\sqrt{4\pi^2+\delta^2}} \tag{2.4}$$

(S. G., Kelly, 2011)

Proper airfoil selection is one of the most significant steps in the wing design process. It is impossible to find a universal airfoil that works in all flight scenarios and airplane configurations. The UAVs wings need to be suited to their working conditions. Their performance can be tested through multiple methods one of which is numerical simulation. XFLR 5 is a free software that allows numerical analysis of airfoils, wings, and whole airframes. This program employs the Vortex Lattice approach (VLM) in conjunction with the 3D Panel Method for wing aerodynamic analysis, and a non-linear lifting line approach for isolated wings. The analysis yields lift and drag coefficients for airfoils and lift and drag forces for wing and airframe simulation. Following the identification of a specific group of profiles corresponding to the assumed requirements, a comparison of aerodynamic properties (lift/drag coefficient) should be performed. Main wing geometrical calculations are the next phase in the UAV design process, which comes after airfoil selection. This type of studies may be performed in "Wing and Plane Design" (one of XFLR 5 modules). During this phase geometrical dimensions of main wing as: span, root and tip chords, twists, dihedrals, and airfoil distribution are established (W. Grodzki et al., 2015).

A wing structure's primary function is to gather up air loads and transfer them to the fuselage. The wing performs the combined function of a beam and a torsion member. It is made up of axial members in stringers, bending members in spars, and shear panels in the cover skin and spar webs. The spar is a heavy beam running span wise to withstand transverse shear loads and span wise bending. Wing ribs are planar structures capable of carrying in-plane loads and are placed chord wise along the wingspan. Ribs, in addition to acting as load distributers, help retain the skin to the contour shape. According to R. Budarapu et al. (2016), due to the symmetry of the wing structure, the semi-wing can be considered in the design calculations. The semi-wing can be can be approximated as a cantilever, whose fixed end is attached to the fuselage. The distance between the front spar and aerodynamic center should be 18-25 percent of the chord length. This prevents torsion and provides sufficient support to the structure. The location of the rear spar should be 55-62 percent of the chord length which renders it sufficient support to the structure (Shiva et al., 2020). As per G. Bramesfeld and R. Prinster (2015), the ribs provide the support for the external skin and restrict it to the desired airfoil shape.

Sandwich composite is a type of composite material formed by bonding two thin, stiff skins to a lightweight thick core. In sandwich composites, the skins carry the majority of in-plane and bending loads, while the core transfers shear and normal loads. (Grodzki, 2015). The study Lamani et al. (2020) found that the balsa wood core structure showcased superior structural strength properties compared to polyurethane foam-based cores. The sandwich composite developed in the research demonstrated satisfactory mechanical properties suitable for UAV applications.

Airfoil selection, geometrical calculations, structural design, material selection, numerical analysis, and manufacturing are all steps in the design of an unmanned aerial vehicle's wing. The primary goal of the wing development process is to create structures that are both strong and light (W. Grodzki et al., 2015). The tapered wing in combination with the multi-element airfoil has issues that directly affects flight safety due to difficulty of mounting the second elements accurately on its designed axis, leading to unsymmetric control surface deflections, so an early decision should be made to favor a rectangle wing (M. El Adawy, 2023). The use of advanced composite materials offers the designer the opportunity to tailor the individual wing components to achieve the desired vibration and aeroelastic characteristics while reducing structural weight (J. Simsiriwong et. al., 2012).

In summary, the design and characterization of a fiberglass wing for a UAV requires careful consideration of various factors such as flight requirements, structural requirements, and cost.

2.2 Finite Element Analysis

Finite Element Analysis (FEA) is a numerical simulation method that generates a mathematical model of a physical system. A structural model is built by applying material properties and applicable boundary conditions, which is referred to as analytical pre-processing. It is followed by the solution of that mathematical representation, which is referred to as solving. Finally, the study of the results of that solution and plotting virtual representations of the results are collectively referred to as post-processing (S. Srividhya et al., 2015). The article by V. Pungoti et al. (2014) states that FEA can help to evaluate the structural performance of the wing under different loading conditions. A.M. Mabbrur et al. (2019) states that supporting boundary condition is also applied in the model. The boundary condition for the model is set to

point where the spar is attached to the fuselage. The authors P. A. pandu, and D. A. Sawanti (2017) have conducted an experimental evaluation and study on composite materials that are reinforced by glass fiber under mechanical loading using FEA software.

By simulating these conditions, areas of the wing that are likely to experience high stress or deformation can be identified and the design to can be adjusted improve its performance and durability. Several studies have investigated the use of FEA for analyzing the structural behavior of aircraft components, such as wings and fuselages. However, relatively few studies have focused on the use of FEA in combination with a whippletree mechanism for structural testing of fiberglass wings.

Overall, FEA can be a valuable tool for confirming the design of a component or system, providing designers with a detailed understanding of its structural behavior, and helping to identify potential design flaws or weaknesses. FEA evaluation helps to ensure the performance of design and confirm it meets the required specifications and is optimized for its intended use conditions. R. Sullivan et al. (2014) highlights the importance of accurate finite element analysis (FEA) predictions and thorough testing in the design and optimization of lightweight composite structures for aerospace applications.

In the paper "Structural Analysis and Testing of an Ultralight Unmanned-Aerial-Vehicle Carbon-Composite Wing", the authors of R. Sullivan et al. (2014) have presented a detailed analysis of the structural performance of an ultralight carbon-composite wing designed for a UAV. The research highlights the importance of accurate finite element analysis (FEA) predictions and thorough testing in the design and optimization of lightweight composite structures for aerospace applications. Before putting any flying object in the air, its airworthiness capabilities must be proven, both to prevent critical damage of the aircraft as well as potential material losses on the ground. As per A. Kurnyta et al. (2020), the first experimental step to verify structural strength is static loading tests, performed on the ground.

Figure 2.2 shows the nature of lift distribution for a rectangular wing section. Lift force is highest near the wing root and gradually decreases as we move towards the wingtip.

The rate of decrement is very low till the three fourth length from the root. Then, lift force generation decreases rapidly near the tip due to wingtip vertices.

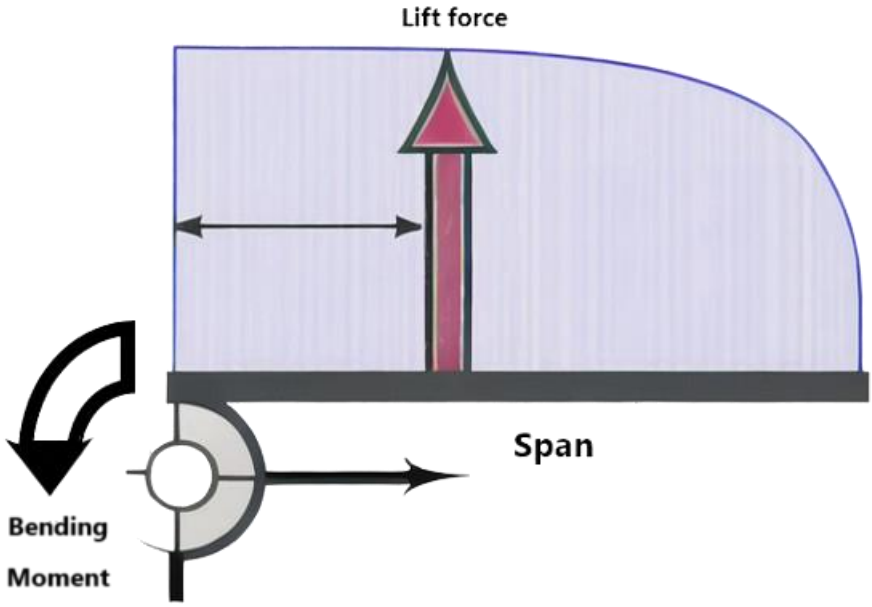

Figure 2.2: Distribution-of-aerodynamic loads over half span of a rectangular wing

2.3 Fabrication and Assembly.

Due to the high strength-to-weight requirements of modern UAV composite materials, polymer matrix composites reinforced with continuous fibers are the best choice. These materials are characterized by young's module twice as high compared to aluminum alloys while retaining two times lower weight (W. Grodzki et al., 2015). As per V. Pungoti et al. (2014), epoxy resin are those resins prepared from compounds containing an average of more than one epoxy group per molecule and capable of being converted through these groups to useful thermosetting products. The advantages of the epoxy resins are low shrinkage, durability, high adhesive, etc. Many factors must be considered when designing a fiber-reinforced composite. Glass fibers usage for reinforcement was pioneered in replacement of metals and used for both commercial and military use. According to the authors of W. Grodzki et al. (2015), polymer matrix composites used in aviation are typically found as symmetrical and asymmetrical laminates. Laminates are layers of fibrous composites bonded together to provide required engineering properties such as strength, stiffness, weight, and so on. The

orientation of the laminate layers has a considerable impact on its qualities. One method for manufacturing engineering composites is hand layup.

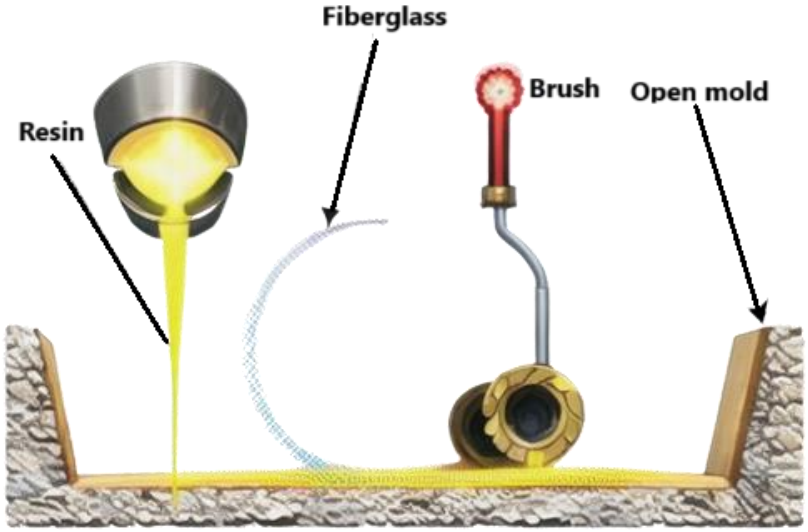

Figure 2.3: Schematics of hand layup of fiberglass over mold

Hand layup is where sheets of fibers, or plies, are placed in a mold by hand and impregnated with a resin. Hand layup of the fiberglass mat and resin on a mold, and curing of the composite under controlled environment is required (J. M. Jablonski, 2021). Fiberglass/epoxy composite laminates are thought to be superior because they perform better under out-of-plane loading than carbon/epoxy laminates, which perform well under in-plane loading (C. G. S. Chandekar, 2010). The design of a wing with a fiberglass composite skin and carbon fiber rods for spars provides a balance of strength, weight, and durability. Fiberglass composite skins provide durability and resistance to fatigue and impact damage, while carbon fiber rods increase overall strength and stiffness. The use of fiberglass/epoxy composite laminates is preferred over carbon/epoxy laminates as they show superior performance under out-of-plane loading.

In the paper “Structural Analysis and Optimization of a UAV wing” the author J. F. M. A. Ferreira (2018) has described steps to involved in building an aircraft wing using carbon-epoxy materials. The use of composite materials, such as fiberglass/epoxy and carbon fiber rods, can provide a balance of strength, weight, and durability. The process of manufacturing fiberglass wings can involve hand layup. Additionally, accurate finite

element analysis and thorough structural testing are essential to ensure airworthiness capabilities.

Aside from the fact that laminated composite materials are employed in demanding industries such as aeronautics and automobiles, they have several drawbacks. The main concerned is about a phenomenon called delamination (separation between the laminas), that can be a caused by mismatch of material properties between layers and the shear stresses produced between them. Fiber debonding (separation of the fiber from the matrix) is a comparable issue that can occur. Other flaws may be introduced during the production of these composite materials. “Interlaminar voids, incorrect orientation, damaged fibers and variation in thickness” are some examples of these (J. F. M. A. Ferreira, 2018).

The paper Lamani et al. (2020) delves into the study of analysis, fabrication, and testing of a lightweight sandwich composite made by balsa wood core and fiber-glass/polyester resin for a UAV wing. The research emphasizes the significance of materials in engineering processes, especially in the aviation sector where weight plays a pivotal role. The sandwich structure, known for its high flexural strength, is essential for a wing to counteract bending loads. The study found that the balsa wood core structure showcased superior structural strength properties compared to polyurethane foam-based cores. The sandwich composite developed in the research demonstrated satisfactory mechanical properties suitable for UAV applications.

The authors of M. J. Sharba et al. (2016). found that the type of resin used also had a significant impact on the properties of the composite. Epoxy resin composites had the highest tensile and flexural strength, followed by unsaturated polyester and vinyl ester composites.

Laminar Composites type composite material with sandwich structure is the latest composite material and is widely applied as a UAV wing structure. Laminar composites and sandwiches consisting of various materials such as Balsa wood fiberglass and polyester resin, Carbon matrix composites reinforced with continuing fibers, Polymer matrix composites, E-glass/Epoxy, Kevlar/Epoxy, Carbon/Epoxy, woven fabrics, etc. This laminar-type composite material with a sandwich structure has good test values and can be used as a UAV wing structure material (Utami et al., 2022).

Research has consistently demonstrated the positive impact of vacuum bagging on the mechanical properties of fiberglass composites and shown its superiority to other manufacturing techniques. K. Abdurohman et al. (2018) has compared the hand lay-up, vacuum infusion, and vacuum bagging methods for manufacturing E-glass composites. The mechanical properties of the composites were evaluated using tensile strength, flexural strength, and impact strength tests. The results showed that the vacuum bagging method produced the highest mechanical properties, followed by the vacuum infusion method and the hand lay-up method. The vacuum bagging method also produced the most uniform surface finish. The literatures led to the conclusion that vacuum bagging provides the highest value of tensile strength of all techniques to manufacture fiberglass due to effective removal of air bubbles and voids, which can weaken the material. Additionally, it provides high stiffness, surface finish and enhanced fire-resistant properties as well.

2.4 Experimental Testing and Data Collection

The study and measurement of the dynamic response of structures and/or fluids to vibration excitation is known as vibration analysis. Traditional modal analysis techniques are either prohibitively expensive, necessitate a complex setup, or both. Low-cost, non-contact measuring devices, such as high-speed cameras combined with computer vision techniques, have been demonstrated to be a viable alternative method for measuring vibrations in structures. Non-contact or non-intrusive optical methods, as opposed to accelerometers, have the advantage of not interfering with the resonance frequencies of the measured structure, which is especially useful when measuring lightweight structures. (W. Zhang et al, 2021).

Modal or vibration testing is now a standard test procedure in the design and development of most engineering systems that may be subjected to dynamic loading. It is commonly used to determine the modal properties of structures in order to eliminate or reduce unwanted vibrations. With the theoretical formulation of vibration test methodologies and the commercial availability of measuring equipment for dynamic testing in the 1960s, modern experimental modal analysis was established (A. Kurnyta, 2020). Ground vibration testing of full-scale air vehicles and aircraft components is typically done with steady-state or transient (impact or burst random) excitation functions. (J. Simsiriwong, 2009).

The data collection system measures the frequency responses of the wing by processing the values of deflection under a given time domain. Obtaining the various vibration modes (and their shapes) and adding them together yields the FRF, so the goal is to find these modes. This is normally accomplished by physically exciting the structure at various frequencies and then measuring how it responds to them. The most common excitation methods are impact hammers and shakers. The first involves striking the structure of interest with a special hammer that contains a force load measuring unit in order to excite its natural vibration modes (Wikipedia, 2023). The impact hammer is used to deliver a quick and sharp impulse to the structure. By minimizing the period of contact, one can ensure that most of the energy is transferred to the structure during the short impact. This helps in exciting the structure at a specific frequency without causing excessive energy transfer, which could lead to unwanted vibrations or inaccuracies in the measurements.

By reducing the mass of the hammer tip, the hammer touches the structure for a shorter period of time. Because the reduced mass allows the hammer to easily reverse direction after striking the structure, the contact time is reduced. Increasing the stiffness of the tip allows the hammer to make contact for a shorter period of time. A rubber tip, for example, could be replaced with a metal tip. A hard tip has a very short pulse and excites a wide frequency range. A soft tip, on the other hand, has a long pulse and excites a narrow frequency range. (gfai tech GmbH, 2023).

Monitoring the vibrations of mechanical components is one of the most important aspects of the proper operation of technical objects. A significant proportion of the research methods in this regard are currently based on the conversion of vibrations using sensors providing data from individual locations. Due to the rapid development of visual systems, new methods for acquiring information on the condition of the object have emerged in parallel with the continuous improvement of these tools. Their actual effectiveness was the deciding factor in the transition from research laboratories to actual industrial installations. In many cases, the use of visualization methods can supplement and, under certain conditions, effectively replace traditional methods. The decisive factor is their non-contact nature and the possibility for simultaneous observation of multiple points of the selected area (Śmieja et al., 2021)

To collect data visual methods employing use of high-speed camera can be employed. The deflection and strain rate can be calculated by this method. Auxiliary equipment used for visual data collection may include cameras, impact hammer, lighting equipment, and marking tools. Video and photos can be captured with proper illumination of the structure which can provide the value of deflection. The process of collecting data also involves inspecting the surface of the wing structure using marking tools to mark any areas of interest, capturing images and videos of the wing structure, and repeating the inspection and data collection process for multiple angles and positions.

CHAPTER THREE: METHODOLOGY

This chapter explains the comprehensive methodology used from the beginning to the end of the project, organizing the methods into different stages. The detailed formulation of methodology, highlighting a quantitative approach, is shown in figure 3.1, depicting the details of the research development.

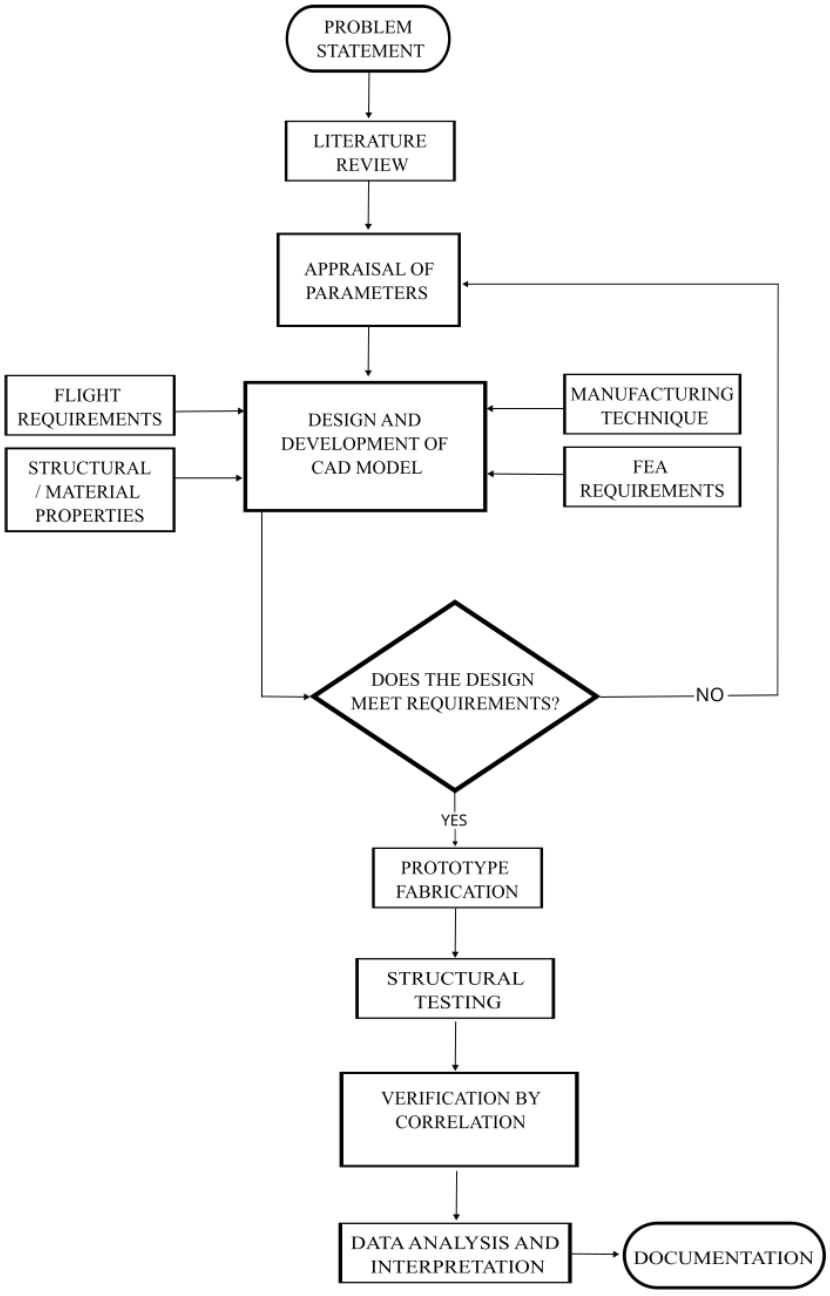

Figure 3.1: Design and validation flowchart

3.1 Selection and Design of Wing

The wing, as an integral component of any UAV, plays a pivotal role in determining its flight characteristics. This section elaborates on the design parameters and considerations that went into the creation of the wing for this specific UAV.

1. Flight Requirements: The study is done considering the aerodynamic properties at cruise flight for a rectangular glider wing design (Eppler 205 airfoil).

2. Wing Dimensions and Characteristics:

i. Span and Chord: The wing has a half span of 56.4 cm and a root chord dimension of 17.25 cm.
ii. Airfoil Thickness: Maximum thickness is 1.80 cm at the root section

3. Structural Components and Design:

i. Primary Structure: The FE idealization of the wing's primary structure includes balsa ribs, upper and lower fiberglass composite skins, two rectangular balsa spars and two cylindrical carbon fiber spars.
ii. Spar Placement: Positioned at 25 percent and 55 percent of the chord length, the rectangular spars are strategically located near the aerodynamic center, as suggested by A. Wood (2023). This placement ensures optimal load distribution and minimizes torsional effects. They serve two purpose, structural reinforcement and as attachment points for the fiberglass composite skin.
iii. Cylindrical spar: Cylindrical spars with a radius of (6*4 cm) provide additional structural support.
iv. Ribs: Ribs of 5mm thickness are place equidistantly across the span at 16 positions.

4. Aerodynamic Considerations:

After inserting the geometrical parameters in the aerodynamic simulation software XFLR5, a fixed speed analysis was defined. Simulation in XFLR5 was run by employing Vortex Lattice Method (VLM2) for aerodynamic analysis of wings. The number of panels in span direction was set to 200 and in transverse direction was set to 50 to obtain accurate data points of coefficient of lift. The results of these simulations were considered for design validation and have been presented in results and discussion section in the next chapter.

i. Wing Shape Selection: The airfoil shape of the wing affects its lift and drag characteristics. So Eppler 205 airfoil which is suitable for sustained cruising with high value of lift-to-drag was chosen for this study. Considering literature of S. Sharma (2021), a rectangular wing shape was chosen due to its suitability for non-high-altitude missions and ease of fabrication.

ii. Aerodynamic Center: Located approximately at the quarter chord, this is the point where the wing's moment coefficient remains constant regardless of the angle of attack. Also, as per the suggestion of the author of the article A. wood (2023), it is good design practice to locate the main spar near the aerodynamic center.

iii. Angle of Attack: Although the AOA at liftoff is higher, the angle of attack chosen for study was 5 °. This value was chosen with an intent to study the wing behavior during cruising speed. This is the angle between the wing and the oncoming airflow that produces the most efficient lift-to-drag ratio for the airfoil. At this AOA, the airfoil generates the most lift with the least amount of drag, which allows the glider to fly for longer distances.

iv. Wing Loading: The wing loading, or the mass of the UAV divided by the wing area, determines the size and shape of the wing. Higher wing loading requires a larger wing area to generate sufficient lift, while lower wing loading can allow for a smaller wing.

Wing loading =Mass of UAV/ Area of wing

= mass/ (mean chord*span)

$= 1.2/ ((17.25*112.8) *10^{-4})$

$= 1.2/0.1946$

$= 6.16\ kg/m^2$

v. Aspect Ratio: The aspect ratio is the ratio of the wing span to the wing chord, and affects the lift-to-drag ratio of the wing. Higher aspect ratios result in longer and narrower wings, which are more efficient for high-speed flights. On the other hand, the shortcoming of larger span is that it will be more challenging to maneuver. So, for cruise flight requirement the medium wing span was designated.

Aspect ratio $= (Span)^2/Area$

$= 1.128^2/0.19458$

$= 6.539$

vi. Lift force using CLavg =

CLavg = Lift force / Area * Dynamic pressure

$0.553 = \text{Lift force}/ (0.194*1.225*0.5*15^2)$

Therefore, Lift force = 14.78 N = 1.506 kg

vii. Weight considerations:

Table 3.1 summarizes component weights for an assumed cruise drone system, including a 4-cell lithium-ion battery, brushless DC motor, electronics, propellers, frame, and payload. Total weight is specified as 1200 grams, aiding in weight distribution and design decisions.

Table 3.1: Estimation of UAV weight that can be supported by the wing

Battery (4 cell lithium-ion)	150gm
1700 kv brushless DC motor	50gm
Electronics and sensors (Esc, accelerometers, wiring, gyroscope, radio transmitters)	150gm
Propellers	13.5gm
Frame and wing weight (upper tolerance)	700gm
Camera/payload	140gm
Total weight	**1200 gm**

Above requirements were addressed before moving on to the modelling of the wing. These measurements were chosen based on the optimal balance between load-bearing strength and weight considerations. The table 3.2 given below outlines key details about the Eppler 205 airfoil profiled wing, encompassing geometric dimensions, aerodynamic performance metrics, and corresponding force values. This comprehensive dataset is integral in analyzing the airfoil's aeroelastic behavior and serves as foundational information for informed design approach.

Table 3.2: Characteristics of the wing at 5° AOA

S. No	Characteristics	Values
1.	Airfoil Profile	Eppler 205
2.	Root Chord	17.25 cm
3.	Tip Chord	17.25 cm
4.	Half Span	56.4 cm
5.	Max Lift to Drag Ratio	20.274 at 5° AOA
6.	Aspect Ratio	6.539
7.	Taper Ratio	1
8.	CL max	0.644
9.	Avg CL	0.553
10.	Avg CD	0.027
11.	Lift force (Full span)	14.81 N
12	Drag force	0.28N

5. CAD Modeling:

SOLIDWORKS served as the design platform, and the modelling were tuned for compatibility with digital fabrication and numerical analysis software. This consideration was crucial to ensure the models' adaptability and effectiveness in subsequent stages of production and analysis.

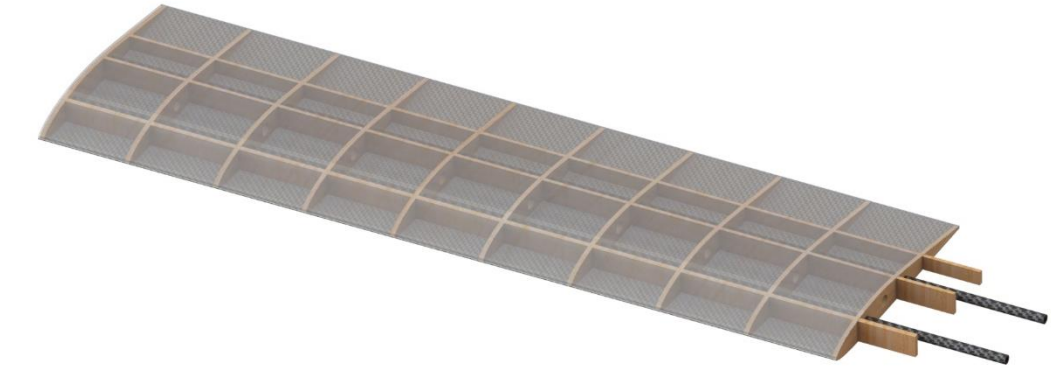

Figure 3.2: Detailed CAD model of the designed wing with 3.175mm thick balsa structures (3D rendered view)

CAD model shown in Figure 3.2 represents the initial design of the semi-wing which incorporated 3.175mm balsa structures, three rectangular balsa spars, two cylindrical carbon fiber spars and 10 ribs positioned along its half-span. Similarly, CAD model shown in Figure 4.2 in the results section represents the improvised design of the semi-wing which incorporated 5mm balsa structures, two rectangular balsa spars, two cylindrical carbon fiber spars and 16 ribs positioned along its half-span. Cylindrical spars with a radius of (6*4 cm) provide additional structural support. Ribs of 5mm thickness are place equidistantly across the span at 16 positions. In this model, spars are positioned at 25 percent and 55 percent of the chord length, the rectangular spars are strategically located near the aerodynamic center, as suggested by A. Wood (2023). The design, especially the size and positioning of the spars, was influenced by literature from Shiva et al. (2020), ensuring the wing's resistance to torsion and providing robust structural support. This placement ensures optimal load distribution and minimizes torsional effects. They serve two purpose, structural reinforcement and as attachment points for the fiberglass composite skin.

3.2 Finite Element Analysis

FEA simulation has been employed to estimate the structural properties of the wing before testing it experimentally. This computational tool was a key component in the design process, as it allowed to simulate how the wing structure would respond under specific boundary conditions. This also allows to anticipate potential stress points or failures before the experimental testing.

The assembly of the composite wing structure were developed using solid SOLIDWORKS software. This model was designed to accurately represent the physical characteristics of the wing, including the shape and size. The geometry of the fiberglass wing assembly, coupled with the wall clamp setup, was imported into ANSYS. Once inside the SpaceClaim environment, necessary adjustments were made to the geometry to ensure compatibility with the subsequent analysis stages. This often involved refining the intersecting regions, removing any redundant elements, and ensuring a clean geometry.

Material properties were then systematically assigned to each element of the assembly. The spar rod was designated as carbon fiber, the skin was defined as fiberglass composite, the skeleton received the properties of balsa wood, and the clamp was set as structural steel. For materials not readily available in the ANSYS material library, custom definitions were created, ensuring that the mechanical properties matched real-world data.

Before proceeding further, the assembly's integrity was verified. Connections between components were checked, ensuring that there were no gaps or overlaps that could compromise the analysis. This step is crucial as the accuracy of load transfer between components depends on these connections.

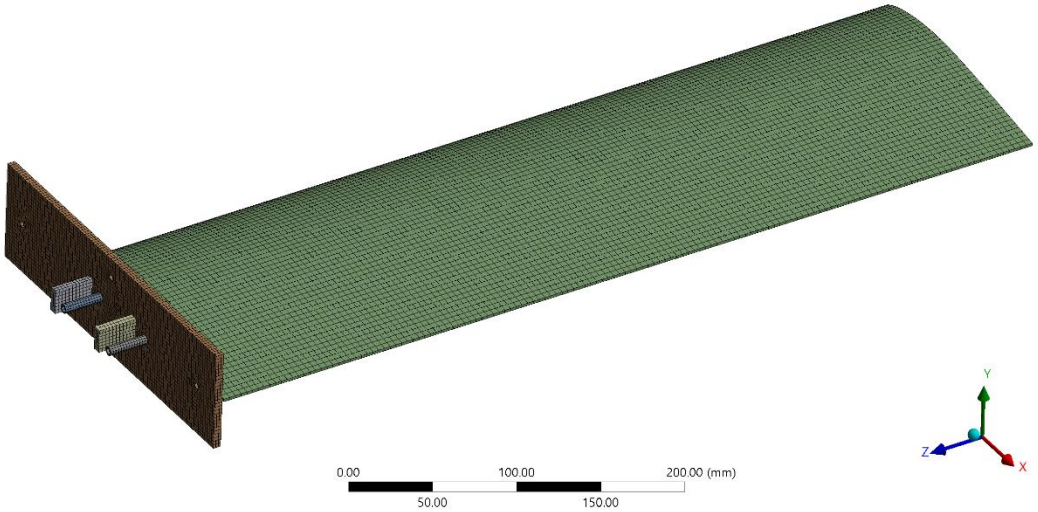

Figure 3.3: Overview of meshing on the entire structure

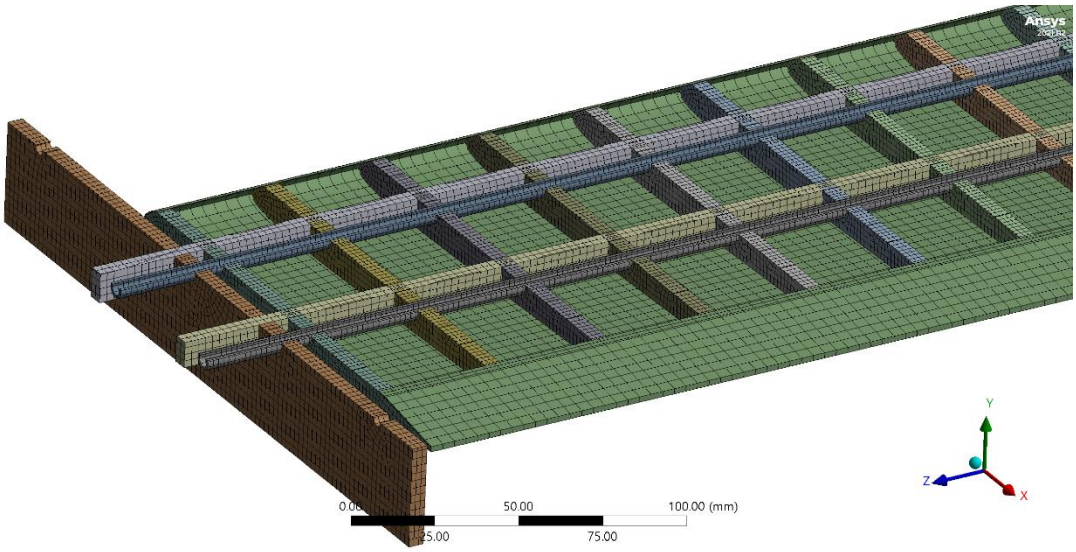

Figure 3.4: Detailed section view of meshing on different components

Given the varied nature of the components, a differentiated meshing approach was adopted. Critical components, especially those with intricate geometries like the spar rods and balsa ribs, were given a finer mesh. The maximum mesh size was 3mm for fiberglass skin and minimum mesh size was 0.6mm for balsa rods. After a few preliminary meshing attempts, an optimal mesh density to accurately represent the geometrical details was achieved, ensuring accuracy without straining computational resources. Figure 3.4 presents more detailed zoomed out view of the differentiated meshing approach employed. There were 63812 mesh elements present along with

354948 nodes. In ANSYS, nodes are points where physical properties are calculated. Mesh elements connect these nodes, breaking the structure into manageable pieces. Elements define the structure's shape and behavior, while nodes enable the calculation of values like stress, strain, and deformation at specific points. Mesh independent test showed that with a 10 percent change in mesh size from the current meshing condition, the accuracy of the results only improved by 0.11 percent.

3.2.1 Structural Analysis Under Limit Load

With the preparatory steps completed, loading and boundary conditions were defined as shown in Figure 3.5. Limit load calculated for the different sections of the span earlier were applied to the corresponding faces, simulating the aerodynamic pressures the wing would experience in flight. Displacement of clamping plate in z direction was set to zero leaving x and y direction to be free. Simultaneously, displacement of rectangular and cylindrical spars in x and y direction were set to zero leaving z direction to be free. In this way the boundary conditions were set to represent the devised design of experimental setup. The analysis settings were then configured. This included setting the appropriate solvers type, setting the numbers of cores to be used, and specifying output parameters. The simulation was subsequently initiated and carried out.

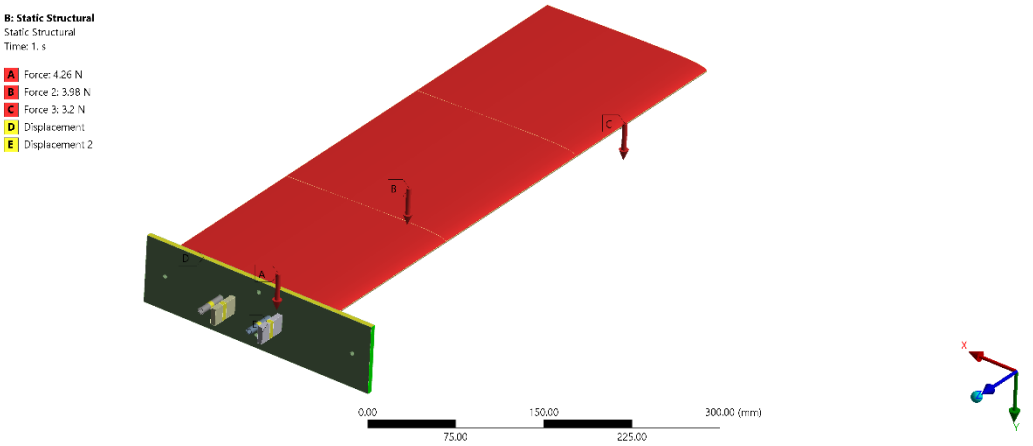

Figure 3.5: Boundary condition and loading condition setup for static structural testing

3.2.2 Modal Analysis Under Limit Load

Modal analysis was conducted for the 5mm balsa design since it shows more promising structural simulation results with lower stress concentration at critical areas and showed

better structural rigidity to loading. Modes representing longitudinal vibration are significant for wings with lower to moderate aspect ratio. So, resulting contour of first vibrations was considered for analysis.

3.3 Fabrication of wing prototype

The fabrication of the UAV wing prototype is a meticulous process that integrates advanced materials and precision engineering techniques. This section describes the step-by-step methodology employed in the creation of the wing.

1. Composite Composition:

As highlighted by J. F. M. A. Ferreira (2018), the bond between fibers and the matrix material is paramount to prevent fiber-related anomalies. Fiber orientation was strategically chosen: fiber cloth with interwoven cross-ply fibers oriented at 45º and 135 º to bear shear loads, while fibers of fiberglass were laid at 90º to handle tensile loads. The combination of these two orientations in a cross-woven pattern ensures that the composite provides enhanced strength and stiffness in both diagonal directions. This is beneficial in UAV application where loads or stresses on wing might be applied off-axis and torsional (twisting) strength is essential. Thus, the wing's structural integrity was fortified by a tri-layered fiberglass composite:

- The exterior layers utilize a cross-ply fiber mat, ensuring resilience against external forces.
- The central layer is exclusively fiberglass, providing rigidity without compromising weight.

2. Scale model development for design verification and material selection:

In line with the prior thesis title, exploration of various combinations of 3D-printed TPU and PLA based internal frame structures, focusing on their strength and flexural rigidity were done. Preliminary scale models developed has been shown in Figure 4.12. Designing these 3D-printed structures demanded careful attention to expansion tolerance.

3. Mold Development:

Use of digital manufacturing tools streamlined the research process ensuring accuracy and the ability to iterate designs rapidly. Digital manufacturing tools shown in the Figure 3.6 includes 3D printers, CNC foam cutters, CNC laser cutter, etc. These have been instrumental in advancing the research on the fiberglass wing. The 3D printer, with its additive manufacturing capabilities, allowed for the rapid prototyping of complex components and fixtures, reducing the time from design to testing. The foam cutter provided the ability to craft accurate foam molds or cores, ensuring the wing's aerodynamic profile was maintained during the fiberglass layering process. Meanwhile, the laser cutter's high precision ensured that intricate components, vital for both fabrication and structural testing, were produced with exacting detail. Collectively, these digital manufacturing tools streamlined the research process ensuring accuracy and the ability to iterate designs rapidly.

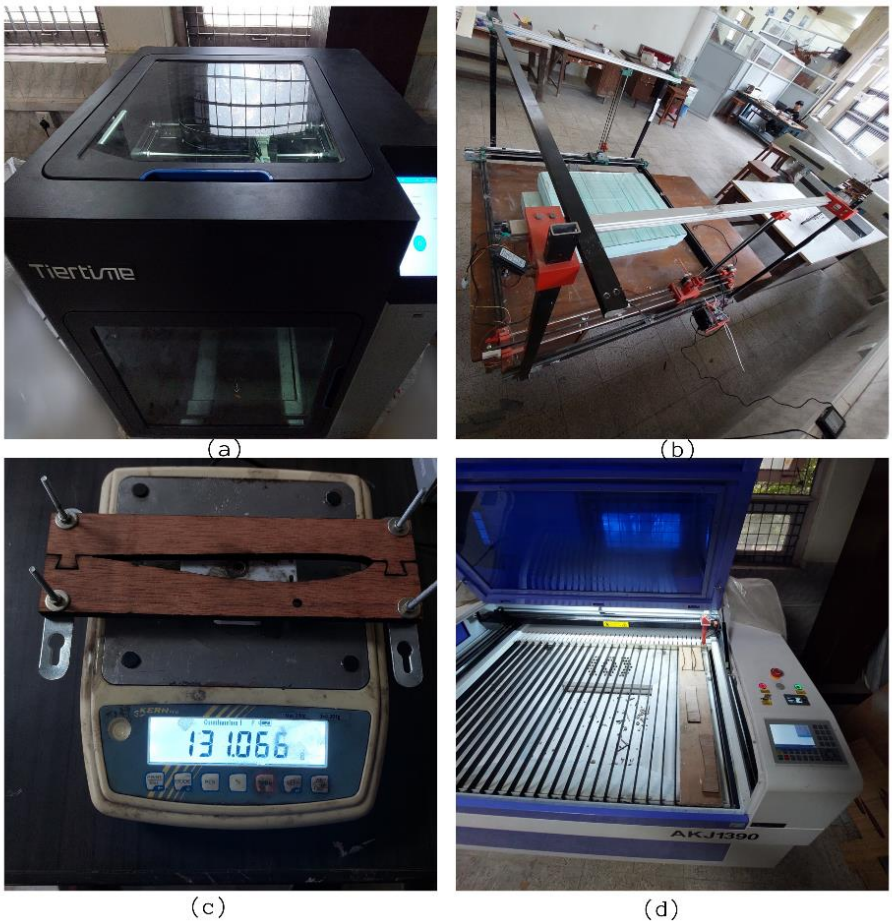

Figure 3.6: Digital Manufacturing tools used for the research (a) FDM 3D-printer (b) CNC Foam Cutter (c) Digital Weighing scale (d) CNC Laser

The foam mold for the wing was crafted using a CNC foam cutter developed in the LAB, with the wing profile's G-code generated via DIYRCWINGS and input into the GRBL HotWire Mega platform. Necessary modifications were made to the hardware to improve its performance and capabilities. Cuts were made along longitudinal direction for easier removal of the foam core from the skin later after curing. Fine sanding was performed on the foam mold as required. Hand layup technique was employed to layer the fiber cloth, fiberglass, and resin on the foam mold. A demolding layer of polyethylene wrap was placed to ensure seamless removal of the fabricated fiberglass skin later.

4. Layup and Curing of final prototype:

A strategic combination of fiber cloth and fiberglass layers, derived from extensive literature reviews, was employed to fabricate the skin. A GSM fiberglass cloth cut into dimensions suitable for the wing was laid over the foam core wrapped in polyurethane. Z-poxy finishing resin, chosen for its optimal properties, was applied over the fiber cloth layers. Among the options available it had lower viscosity, non-brittle property, suitable working time, and feasible curing time. Calculated mixing of resin was done and was applied over the first layer of the fiber cloth with a fine grade brush. Sufficient setting time of about 20 minutes was provided for the resin and the second layer of 100 GSM fiberglass was laid over. The procedure for applying resin was replicated on the second layer. Any surplus resin was removed using a plastic card. The resin was then left to set for an additional 20 minutes. To achieve a smooth surface finish, the edges were clamped with paper clips, ensuring the layers were adequately stretched. The assembly was then placed in a vacuum bag, and the air was extracted. Vacuum bagging process was crucial for eliminating any trapped air bubbles that could weaken the skin and for ensuring the skin conformed to the foam core, preserving the airfoil shape. It also acted as a barrier against moisture and other environmental elements.

After a 3-hour curing interval, another 30 GSM wing layer was added on top, effectively sandwiching a fiberglass layer between two fiber cloth layers. This specific combination of materials was chosen based on literature reviews. The wing's trailing edge was clamped once more, and another round of vacuum bagging was conducted to cure the top layer. Once the curing process was finished, all clamps were detached. After curing phase was completed, the foam core was meticulously removed, ensuring

the integrity of the fiberglass skin. The foam core was segmented and extracted using the CNC's hot wire, which was positioned between the foam core and the cured fiberglass skin. The final product was inspected to ensure adherence to design specifications. Upon retrieval of the skin, its dimensions were recorded and inspected for discrepancies. The results showed that the measurements were consistent with the intended design. The intermediate processes involved in fabricating the fiberglass wing are shown in Figure 3.7.

5. Balsa Skeleton and Fiberglass Skin Integration:

The frame's design was conceptualized in SolidWorks, exported in DXF format, and further refined using ASPIRE 10.5. The optimized DXF file was then processed in RDWorks V8 for CNC laser cutting. Precision cuts were made using a CNC laser, with design considerations like part bridging and ablation tolerance leading to kerf formation. The assembly process involved inserting the carbon rod into the balsa structure. This was followed by resin application over top and bottom faces of balsa skeleton and insertion into the fiberglass skin for curing. These intermediate steps are highlighted in Figure 3.7 above. 0.5cm length of balsa trailing edge was removed due to its fragility, which posed challenges during assembly. Through iterative processes, both the thickness of the balsa wood and the spar's design were enhanced.

Once the balsa components were assembled and the carbon rod (6 * 4 mm) was integrated, the entire frame was coated with resin. It was then encased within the fiberglass skin for curing. Carbon fiber rods, selected for their unparalleled tensile strength, were integrated as cylindrical spars. The ribs are instrumental in preserving the wing's shape, while the combined strength of the spar and skin ensure majority of the load is supported.

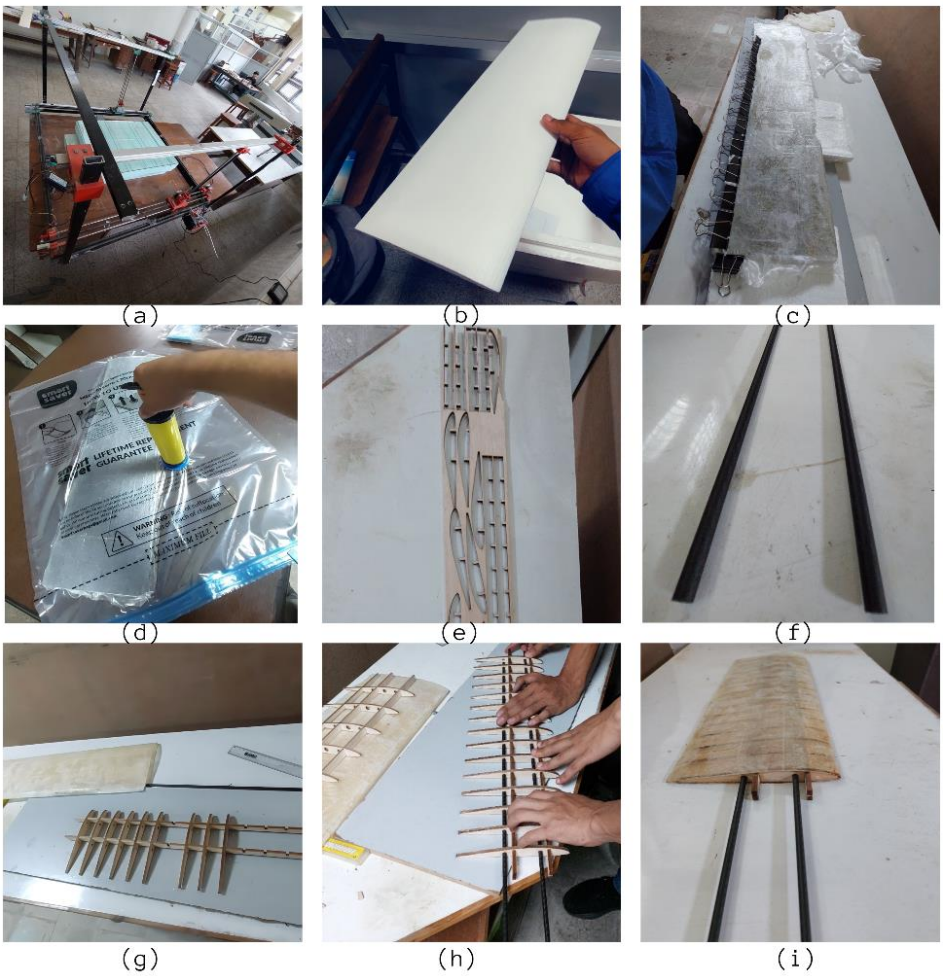

Figure 3.7: The intermediate steps involved in fabricating the fiberglass wing.

(a) CNC foam cutter (b) Fabricated foam mold (c) Layup of fiberglass layers over foam to form skin (d) Vacuum bagging of the skin (e) Laser cut balsa parts (f) carbon fiber rods (g) Assembly of balsa components to form internal frame structure (h) Insertion of carbon rods into the frame structure (i) Assembly of frame and skin

3.4 Test Rig Setup

To check that the wing structure is sufficiently robust to withstand such forces in actual flight, static wing testing involves applying a load equal to the wing design limit load.

Table 3.3: Datapoints (XFLR5) of span and CL for different sections of wing along with the corresponding lift generated.

Span	Corresponding coefficient of lift	Average CL	Lift generated	Loading point (from root)
56.4	0.0178			
55.4	0.16902			
54.4	0.23419			
53.4	0.284			
52.4	0.32			
51.4	0.35			
50.4	0.38			
49.4	0.405			
48.4	0.426			
47.4	0.44			
46.4	0.459			
45.4	0.474			
44.4	0.488			
43.4	0.5			
42.4	0.508			
41.4	0.52			
40.4	0.53			
39.4	0.5368	0.3993584	1.78 N	47 cm
38.4	0.546			
37.4	0.552			
36.4	0.56			
35.4	0.565			
34.4	0.572			
33.4	0.577			
32.4	0.581			
31.4	0.588			
30.4	0.5939333			
29.4	0.5914			
28.4	0.596			
27.4	0.6006			
26.4	0.6034			
25.4	0.606			
24.4	0.611			
23.4	0.613			

22.4	0.616			
21.4	0.62			
20.4	0.623			
19.4	0.626	0.5944912	2.65N	28.2 cm
18.4	0.6274349			
17.4	0.6290311			
16.4	0.632			
15.4	0.633			
14.4	0.634			
13.4	0.635			
12.4	0.638			
11.4	0.638			
10.4	0.638107			
9.4	0.6384			
8.4	0.63907			
7.4	0.64			
6.4	0.6404			
5.4	0.641			
4.4	0.64106			
3.4	0.6438	0.6379254	2.84N	9.4 cm
2.4	0.644			
1.4	0.644			
0.4	0.64428			
Half span = 56.4cm	Average CL= 0.544		Lift (Half span) = 7.27N	

The lift characteristics of the wing's half-span were analyzed. An average of the lift coefficients from various points along this half-span was taken, a process known as spatial averaging. For this the half-span was then divided into three segments, each being 18.8cm in length. An average lift coefficient for each segment was subsequently calculated. Using these averaged coefficients, the lift force for each of the three segments was determined through the analytical method and is tabulated above in table 3.3. To enhance the precision of the analysis, these forces were distributed over four specific points on the half-span. By this method, a clear understanding of the number of loads to be applied at each of these four points, to accurately mimic the wing's real-world load distribution along the half-span, were deduced.

The plot shown by Figure 3.8 illustrates the variation of coefficient of lift along the half span of the wing. This was generated by curve fitting in MATLAB using the data points

extracted from XFLR5. The data from XFLR5 plots in Figure 3.8 below provided both a qualitative and quantitative understanding of aerodynamic loads, ensuring that the wing is tested under realistic and critical conditions. After analyzing the MATLAB plot of the coefficient of lift vs. span from XFLR5, the deduction of the loading point for structural testing was done. The plot shows maximum value at midspan which is the same region where the wing might face the most stress. This analysis was essential for the estimation of the position and loading values in the actual rig.

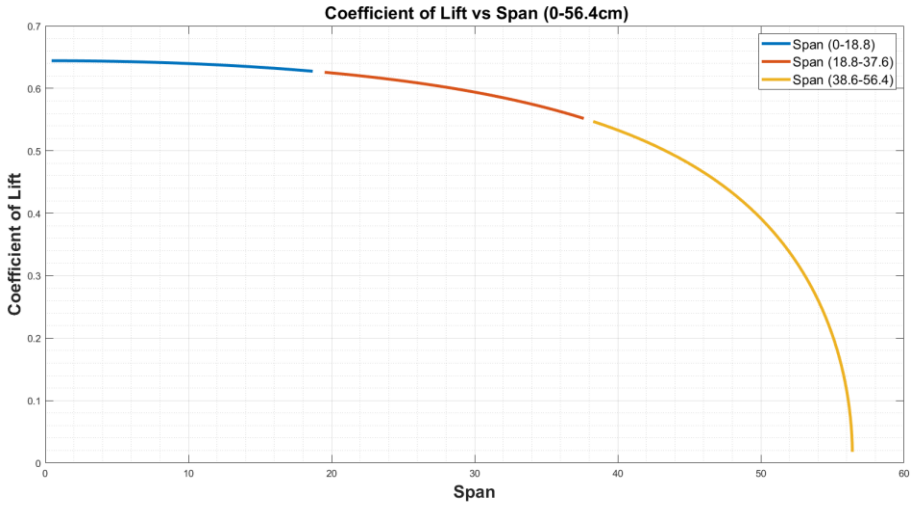

Figure 3.8: Coefficient of lift vs Half-span obtained by plotting XFLR5 datapoints

Creating a 3D-printed scale model (1:2) of a whiffle tree mechanism shown in Figure 3.9 began with the design and conceptualization phase using CAD software, ensuring the design was to scale and mimicked the actual mechanism's geometry. Once the design was finalized, PLA was chosen as the appropriate 3D printing material for its cost-effectiveness and ease of printing. The design was then sliced using software to convert it into layers suitable for 3D printing. After printing all components, they were assembled, ensuring the mechanism could articulate as intended.

The creation of 3D-printed whiffle tree model served several purposes. Firstly, it offered a tangible representation of the whiffle tree mechanism, aiding in visualization and understanding. Furthermore, 3D printing provided a cost-effective and rapid prototyping solution, allowing for design iterations without significant expenses. The model acted as a design verification tool, ensuring all components fit and functioned cohesively and aided in the decision to whether move onto an alternative loading mechanism. In consideration of the intricate and time-intensive fabrication process

associated with the construction of a full-scale Whiffle tree rig, a judicious decision was reached to undertake the experimental investigation utilizing a simplified loading approach. This determination was made after consultations with supervisory experts.

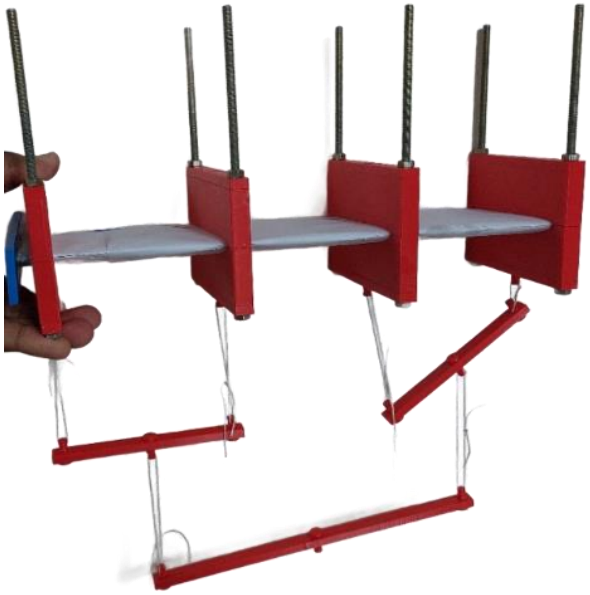

Figure 3.9: 1:2 scale 3D-Printed model of the whiffletree test rig

The experimental setup decided upon involved utilizing a straightforward and sturdy desk provided by the Incubation Lab of IOE, Pulchowk. The desk, featuring rectangular metal tube frames, served as the foundation. The selected configuration of the test rig was much simpler compared to the whiffle tree rig. A precise rectangular cut, carefully executed on a 6mm mild steel plate, was strategically sized to allow the wing's root to smoothly pass across it. Holes, strategically positioned on the plate, facilitated the secure clamping of acrylic plates. This metal plate was seamlessly welded to one side of the desk. Precision was emphasized in the creation of holes and rectangular slots on the acrylic plates using a laser cutter, ensuring an exacting level of tolerance. These meticulously crafted cuts and holes were designed on the acrylic plates to accommodate the insertion of both rectangular balsa spars and cylindrical carbon fiber rods, respectively. This configuration for root fixation was ingeniously devised to authentically emulate the actual clamping mechanism employed when attaching the wing to the fuselage of a UAV.

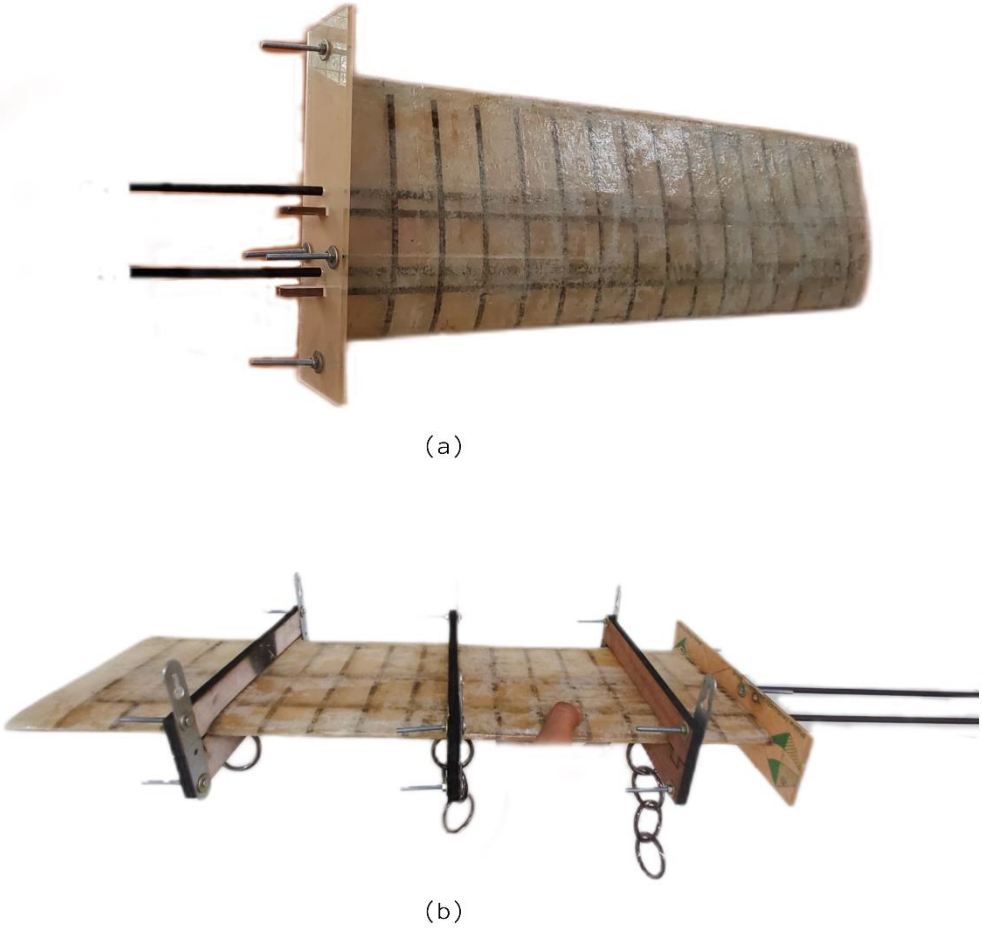

Figure 3.10 (a): Wing prototype with acrylic clamps affixed (b): Wing prototype with acrylic clamps and wooden cradles affixed

Semi-wing approach was employed to perform the static structural testing. The test rig used for the structural testing of the wing consisted of a load application system and a data collection system. The wooden cradles attached to wing surface and the acrylic wall clamp shown in Figure 3.10 were the part of load application system. Similarly, the CHRONOS high-speed camera shown in Figure 3.11 was the major component of data collection system. Other components were lighting setup, camera stands, camera triggers, background board, impact hammer, etc. The load application system incorporated cradles and weights and applied loads to the wing. The load application system was only attached for experiments involving loaded conditions. The test rig was set so as to meet the requirements of the testing, including the loads and the measurement accuracy. The top and bottom pieces of the wooden cradles were made

by laser cutting wood to closely resemble the airfoil shape at the contact surface. Using laser cutting for the airfoil shape guaranteed precision, ensuring the wooden blocks aligned perfectly with design specifications. The wooden cradles were designed and fabricated so as to tightly fit around the wing surface. The cradles were connected to weights representing weights using carabiner hooks. The clamping of the wing was done, onto a rigid metal frame, to mimic the fixed support of root wing. For this a design of the clamp was developed and fabricated to accommodate the fixation of root of the wing specifically the rectangular balsa spars along with the cylindrical carbon spars. The refined design of the clamp was made by laser cutting the geometrical parameters of the clamp onto a 5mm acrylic sheet.

Figure 3.11: Overview of the experimental setup

3.5 Experimental Data Collection

The data collection system consisted of high-speed camera clocked at 250 fps to measure the vibration response of the wing. A strip of black tape was attached to the tip section of the fiberglass wing. The displacement/disturbance was provided to the wing tip using impact hammer with an intent to reduce the contact time. The background of the captured frames was white to bring out contrast in the picture and accurately measure the movement of the wing tip region. Proper lighting setup illumination the white background ensured this. Suitable camera angle was devised and images were taken.

The TIFF data were collected for three repeated readings for each no-load, half load and full-load conditions of the wing setup. Also, dimension/depth estimation was done using a cm scale marking attached to the wing structure. This was used to estimate the pixel density (pixel per mm), thus acting as a reference for finding correct displacement of wing tip. The TIFF data from both experimental modal analysis test and wind tunnel test were processed in MATLAB to find the displacement versus time plots for and the results were further processed for FFT to find the natural frequency of vibration. For each loading condition under modal analysis test, three repeated readings were conducted and analyzed for consistency.

Figure 3.12: Experimental Setup for Wind Tunnel Testing of the Wing

The wind tunnel test was conducted with an intent to obtain the frequency of vibration of the wind at actual aerodynamic loading condition. For this the wing was adjusted at 5° angle of attack and the wind tunnel was operated maximum velocity of 6.5 m/s. From calculations the load value obtained at 6.5m/s wind tunnel velocity with wing positioned at 5 AOA was 2.77N. This load value is equivalent to about 18 percent of fully load value at 5 ° AOA condition. The experimental setup for wind tunnel testing is shown in Figure 3.12.

Understanding modal frequencies and damping properties of a wing structure is essential for preventing resonance, enhancing performance, and putting into practice efficient vibration control strategies. It provides a foundation for monitoring structural health, which enables the early identification of deterioration or damage. Furthermore, overall safety and dependability are improved by the capacity to confirm design standards and guarantee that structures operate within safe dynamic ranges.

CHAPTER FOUR: RESULTS AND DISCUSSION

4.1 Designed wing:

Some of the results of the XFLR5 analysis are lift and drag coefficients along with lift and drag forces for the case of wing and airframe simulation some of which are presented in Figure 4.1. On addition, the other useful data obtained from the simulation was the maximum CL and surface area of the wings.

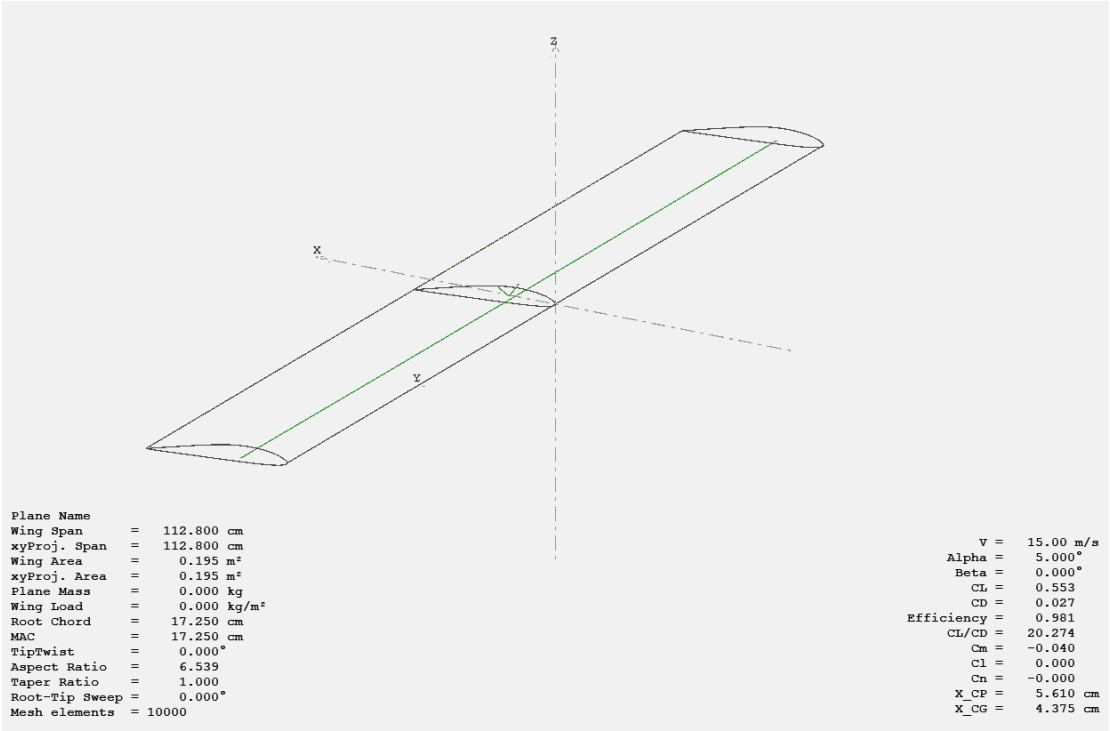

Figure 4.1: Wing design simulation using XFLR5

The characteristics of the wings obtained by analytical calculation along with the results from the XFLR5 simulations have been presented below:

i. The aerodynamic center was obtained at 4.37cm from the leading edge and the angle of attack chosen for study was 5 °.

ii. Eppler 205 airfoil which is suitable for sustained cruising with high value of lift-to-drag was chosen for study. Additionally, wing design was finalized for a rectangular wing.

iii. The wing loading, or the mass of the UAV divided by the wing area is 6.16 kg/m^2.

iv. The aspect ratio is the ratio of the designed wing is 6.539.

v. The maximum lift to drag is 20.274 at 5 ° angle of attack.

vi. Maximum weight of 14.53N can be lifted by the total wing span at 5 ° AOA.

The FE idealization of the improvised wing's primary structure includes balsa ribs, upper and lower fiberglass composite skins, two rectangular balsa spars and two cylindrical carbon fiber spars.

Figure 4.2 is a rendered view of the assembled wing which shows the positioning of the components of the balsa skeleton and carbon fiber spar rod enclosed by the fiberglass skin. There are a total of 16 ribs and two rectangular balsa spar. Further reinforcement is provided by the cylindrical carbon fiber spar. The rectangular spars extend beyond the skin toward the wing root so that both the rectangular and cylindrical spars can be fixed to the fuselage wall. This facilitates better load distribution and improves the structural strength of the wing. This design was finalized further structural simulation and fabrication.

Figure 4.2: CAD model of the designed wing with 5mm thick balsa structures (3D rendered view)

4.2 FEA results:

4.2.1 Results from structural analysis:

Upon completion, a range of results were obtained. Metrics such as total deformation, stress, and strain were reviewed. The earlier design model featured three rectangular spars positioned along Simulation run on earlier model incorporating 3.175 mm thick balsa indicated potential stress concentration on the connecting position of rear most spar and ribs. The total deformation for wing with 5mm balsa structure was 4.42 mm Which is reduction in the deformation value by about 15 percent compared to wing with 3.175mm balsa structures.

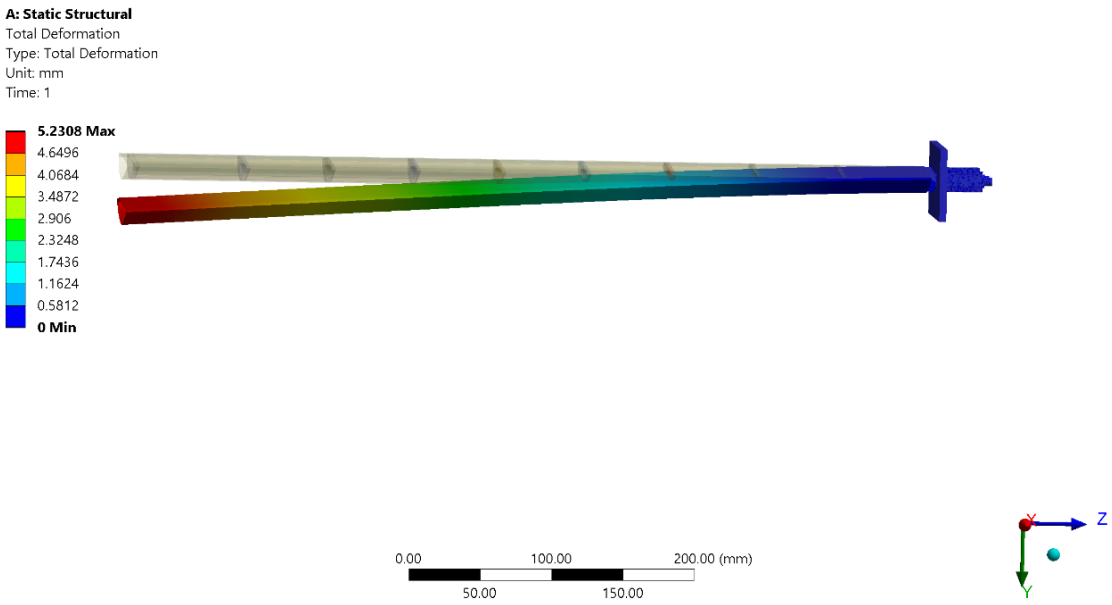

Figure 4.4: Total deformation contour under limit load (3.175mm balsa structures)

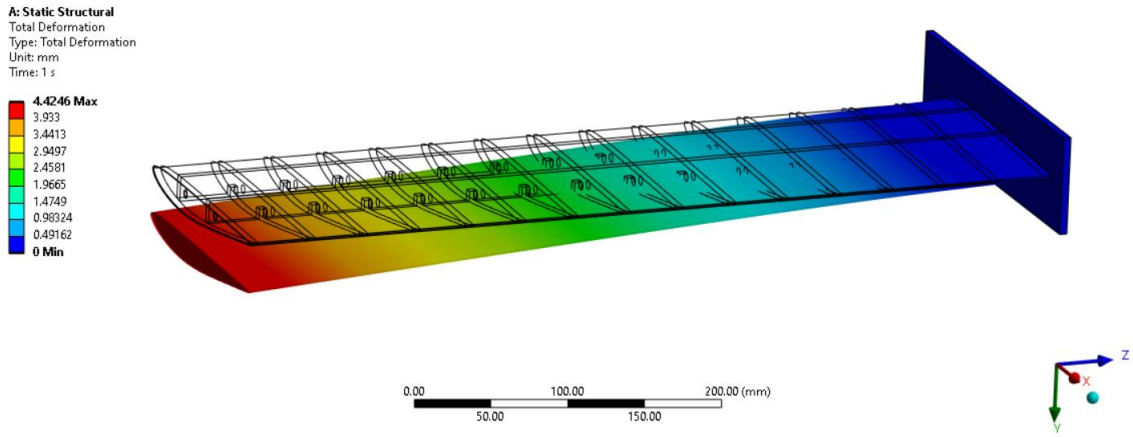

Figure 4.5: Total deformation contour under limit load (5mm balsa structures)

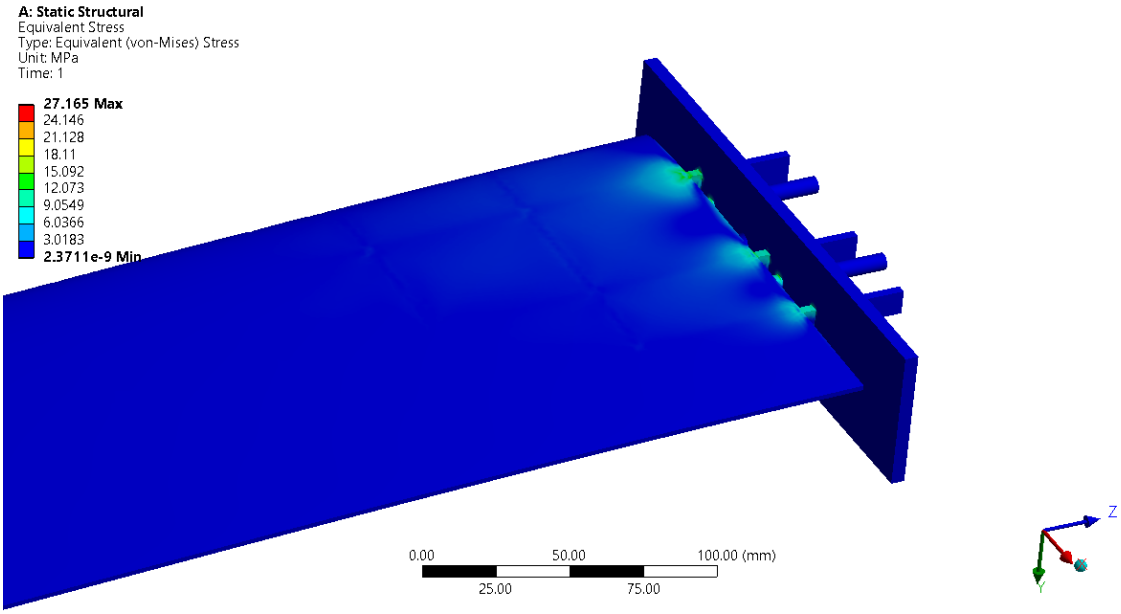

Figure 4.6: Equivalent stress contour under limit load (3.175mm balsa structures)

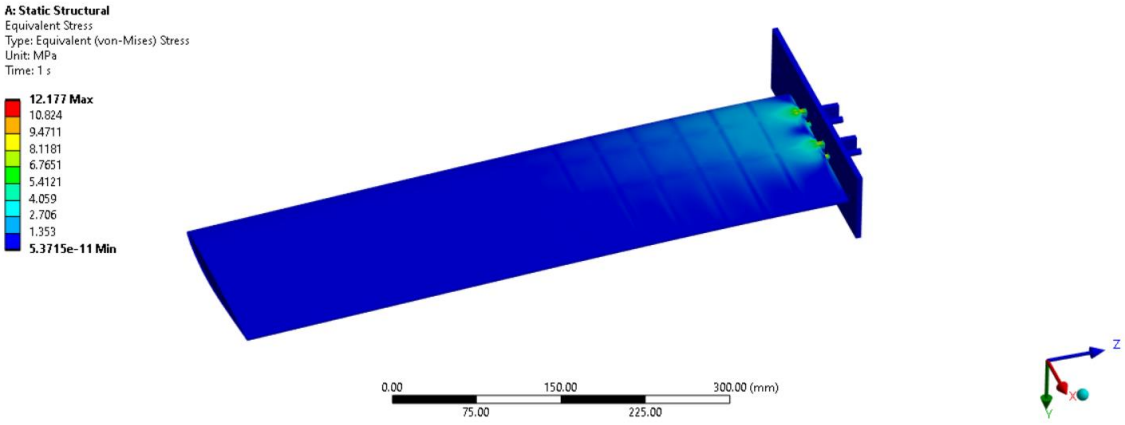

Figure 4.7: Equivalent stress contour under limit load (5mm balsa structures)

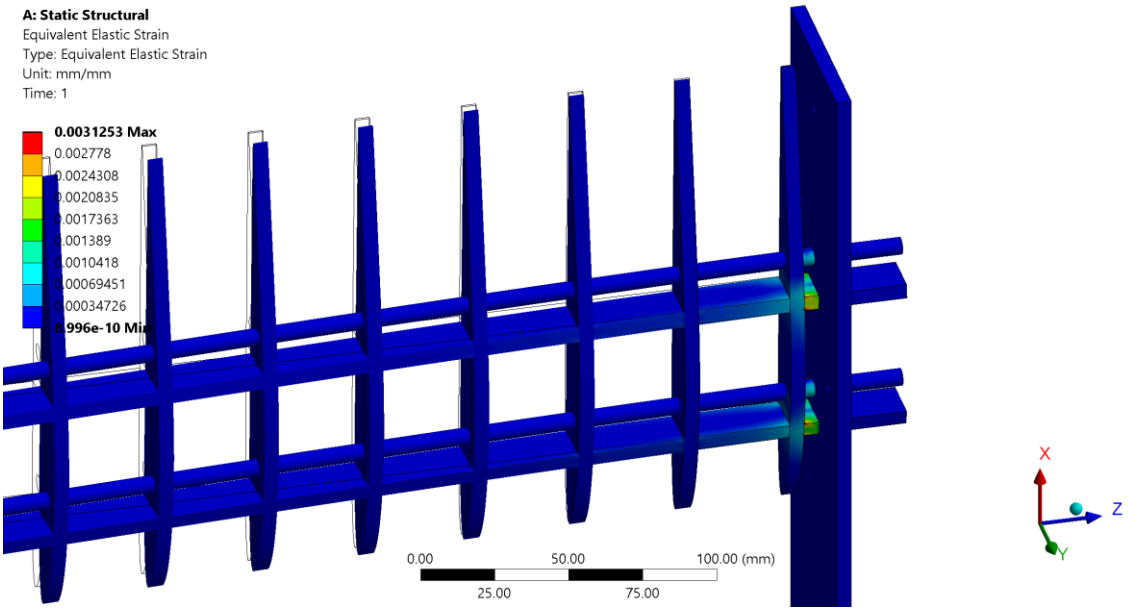

Figure 4.8: Contour plot highlighting regions of high equivalent elastic strain ((5mm balsa structures)

Deformation and stress metrics informed design tweaks such as adjusting spar count and component thickness. Design modifications were made for stress areas like trailing edge. As a result, the stress and strain on the refined design was reduced by 55.2 percent and 63.2 percent respectively with the only downside being 10.34 percent increase in total weight of the wing.

Significant wing flex or shape change can result in instability and decreased control, making it challenging for the pilot to steer the aircraft safely. So, lower deformation values show better structural rigidity of wing to loading. Based on this insight, the design was modified to incorporate only two rectangular spar, 16 ribs and the thickness of balsa components was increased to 5mm.

4.2.2. Results from modal analysis:

Aerodynamic load can impact the distribution of mass and stiffness in the structure by deforming the wing. Changes in mass distribution and stiffness can alter the natural frequency. The vibration characteristics of the wing structures are studied by modal analysis as well as experimental setup to find the natural frequency of the wing structures. For both numerical & experimental state we considered the aircraft wing as cantilevered beam where root is fixed & the tip is free.

The result of the structural analysis was used in modal analysis system and mode shapes representing the longitudinal deflections were obtained. The first longitudinal mode shape resulting from the modal analysis is shown in Figure 4.9. It represents longitudinal deflection and is located at 18.014 Hz of frequency. There is single stationary node present in the first mode shape located towards the fixed end of the structure. The regions displayed in blue color indicate the location of stationary nodes. Similarly, from the resulting contours for first longitudinal mode at half load and full load, the modal frequencies obtained were 12.06 Hz and 9.97 Hz, are also presented in Figure 4.10 and 4.11 respectively.

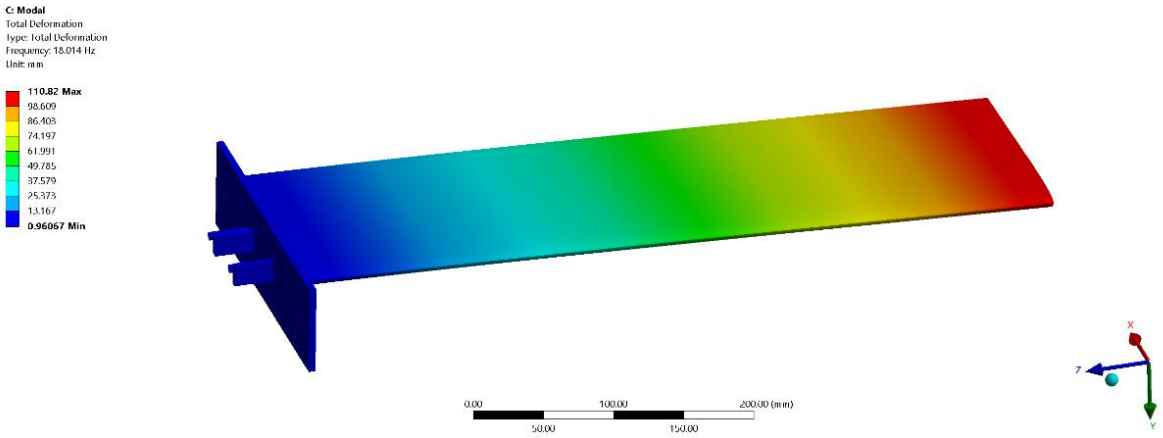

Figure 4.9: Resulting contour of first longitudinal mode of vibration at no load condition

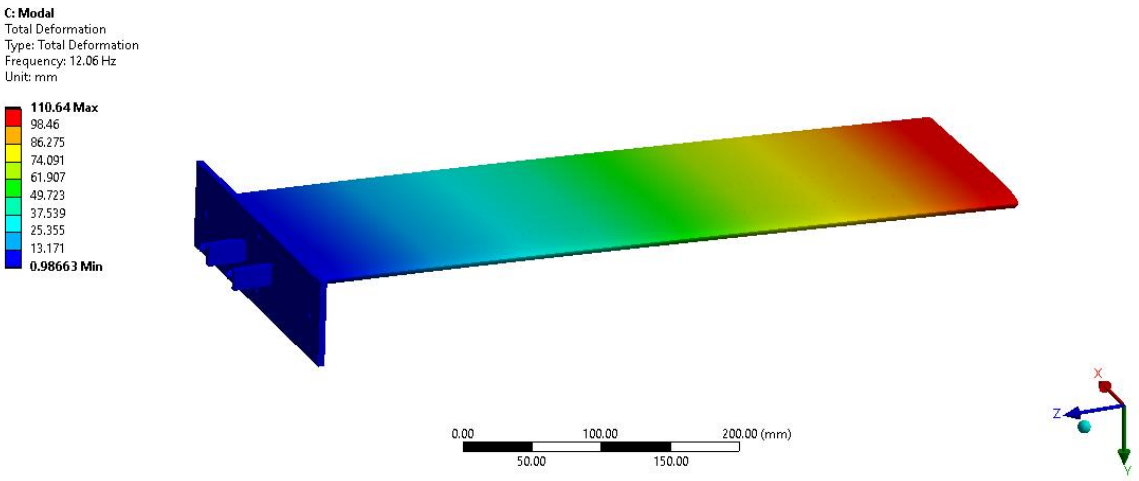

Figure 4.10: Resulting contour of first longitudinal mode of vibration at half load condition

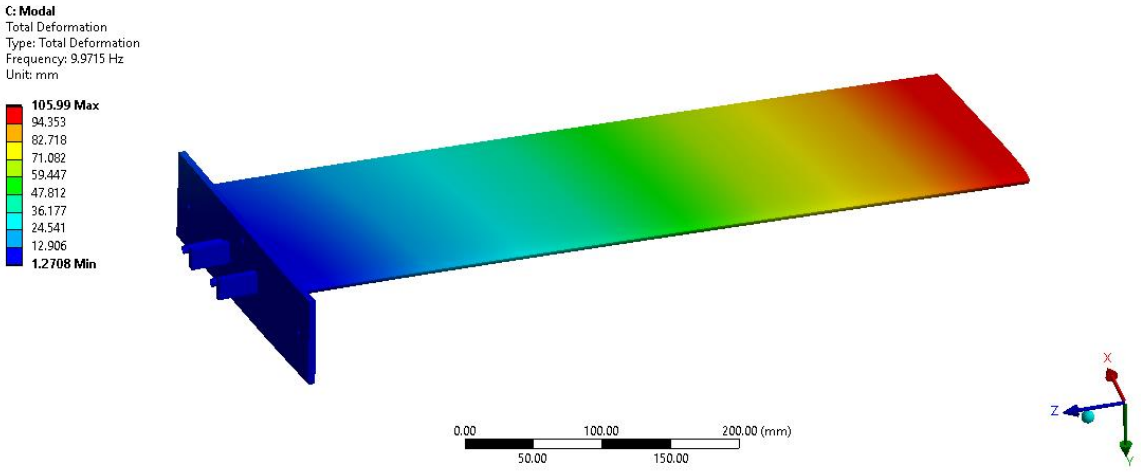

Figure 4.11: Resulting contour of first longitudinal mode of vibration at full load condition

The values of deformation obtained from modal analysis can provide a relative measure of deformation among different mode shapes. Modal analysis yields information about how a structure deforms in response to various vibration modes, and it quantifies the deformation characteristics for each mode. Comparing the deformation values across different mode shapes allows to understand which modes induce larger or smaller deformations in various parts of the structure. This information can be valuable for design and analysis purposes, helping to identify critical modes or areas of concern where deformations are more pronounced.

The modal analysis simulation indicates a substantial reduction in the wing's natural frequency with incremental weight additions. This observation implies a potential shift in the structural response as loading intensifies. Specifically, heavier loads correspond to a constrained oscillation frequency, suggesting altered dynamic behavior. At the same time, in the presence of strong wind forces, the engine must operate at an increased speed. This phenomenon indicates enhanced structural stability, reducing the likelihood of excessive oscillations and fatigue under heavy loads due to the difference in frequency response range between wing structure and propulsion system. The comprehension of these dynamic characteristics is necessary to ensure the structural integrity and longevity of the wing. A detailed comparative analysis of the results is provided in the subsequent discussion section.

4.3 Fabricated wing prototype:

The Computer Aided Design Tools have been employed extensively for standardized design and manufacturing of the wing. Various materials were scrutinized and tested, leading in the final material selection.

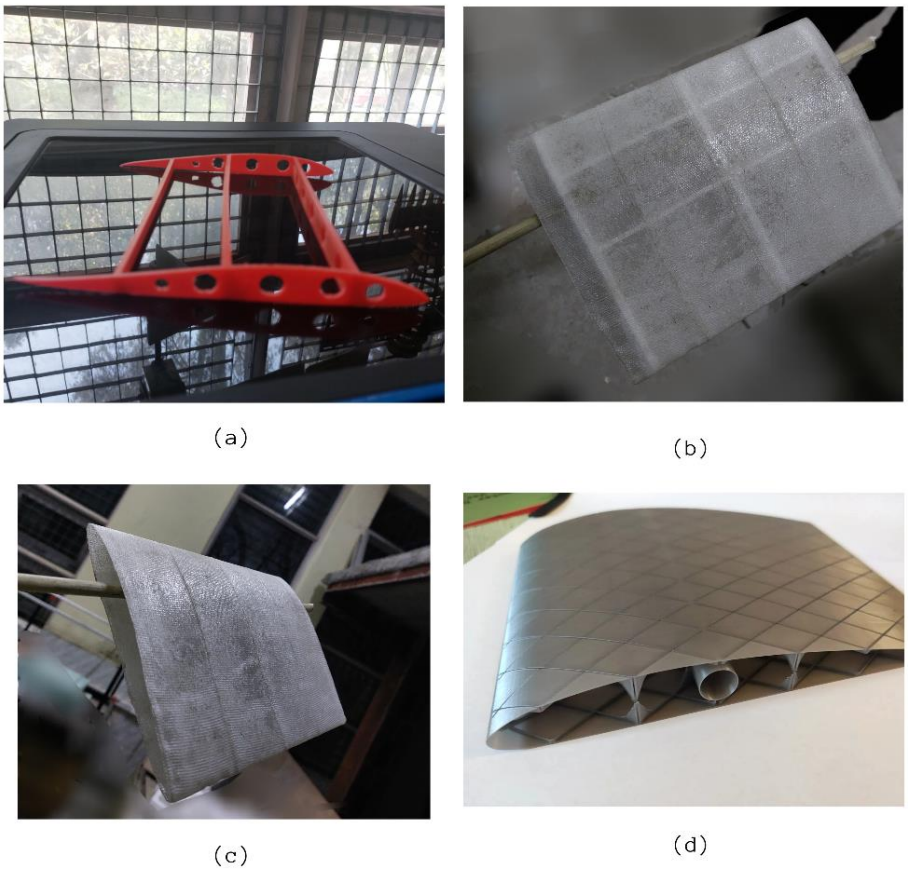

Figure 4.12 (a): Modular frame structure fabricated by 3D printing TPU

(b)/(c): Scale model incorporating fiberglass skin on 3D-printed TPU frame structures

(d): Wing section made by 3D printing PLA

The initial exploration of 3D-printed components informed on important aspects of the wing design. While 3D-printed TPU structures exhibited flexural rigidity deficiencies, PLA structures, on the other hand, lacked the desired fatigue resistance and often resulted in cracked failures. The assessment of initially constructed scale model for its loading characteristics did not align with the deflection criteria and showed large deflection. Additionally, maintaining the wing's weight limit proved challenging when utilizing these materials. Hence material selection, informed by scrutiny and testing, favored balsa wood over a 3D-printed polymer for the skeleton structure. Also, the

design parameters like component thickness, numbers of spars and ribs, etc. were refined. Given the challenges with 3D-printed materials, a modular internal frame structure comprising balsa ribs, rectangular balsa spars, and carbon fiber rod spars was finalized for design and production. The finalized semi-wing, weighing 175gm, contributes to a total wing weight of 350gm, well within the acceptable range for the intended UAV design.

The fabricated wing skin was inspected to ensure adherence to design specifications. Upon retrieval of the skin, its dimensions were recorded and inspected for discrepancies. The results showed that the measurements were consistent with the intended design. The resulting wing after the integration of skin with internal frame structures has been presented in Figure 4.13 below.

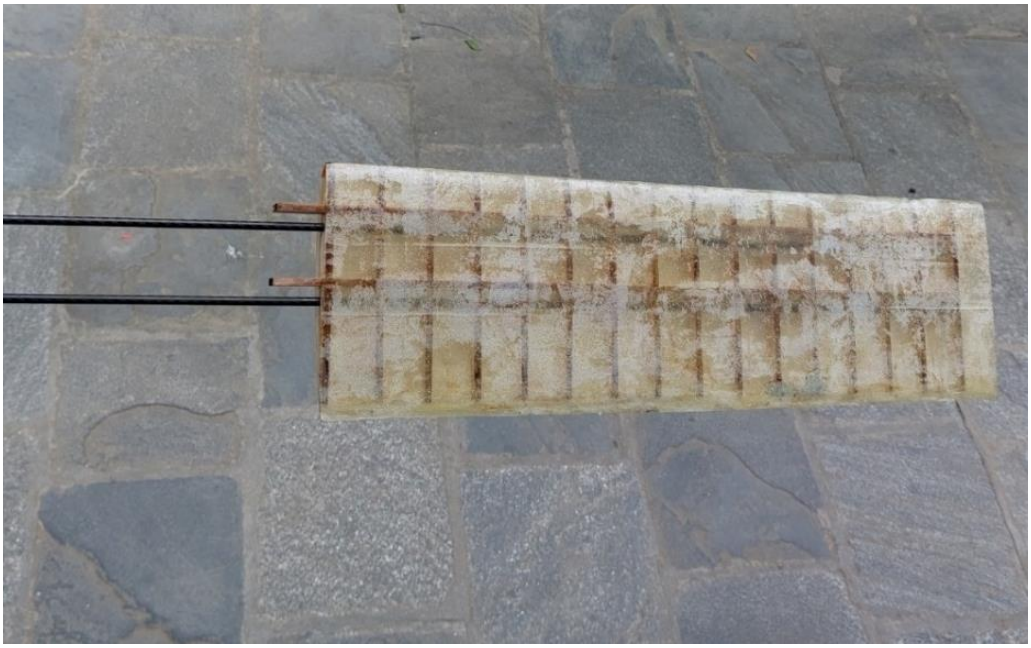

Figure 4.13: Fabricated wing prototype ready for testing

4.4 Test rig:

The total lift force applied on the overall wing span at wind speed of 15m/s for an AOA of 5 ° was determined to be 14.81 N using XFLR5 software. After deducting the drag force value of 0.28N from obtained lift force the usable lift was found to 14.53N. Using the half wing loading value of 7.27 N as limit load, the ultimate load to be applied was found to be to the half wing is 7.27*1.5=10.905N (the ultimate factor is 1.5). In a similar manner the loading values for half load condition was determined to be 5.45N. Figure 4.14 shows the working overview of the experimental modal analysis system.

Figure 4.14: Motion capture setup taking readings

4.5 Analysis of Experimental Data:

4.5.1 Experimental Modal Analysis:

The digital motion capture analysis employed for experimental structural testing demonstrated notable advantages in terms of efficiency, versatility and accessories compared to conventional transducer-based measurement techniques.

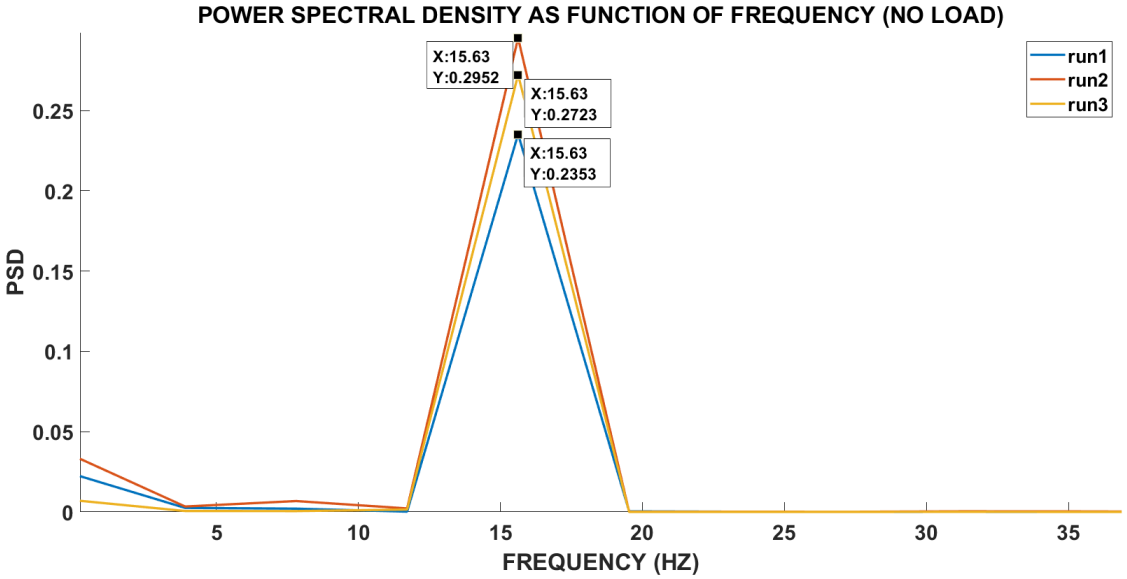

Figure 4.15: PSD as function of frequency for three repeated readings for no-load condition (FFT plot)

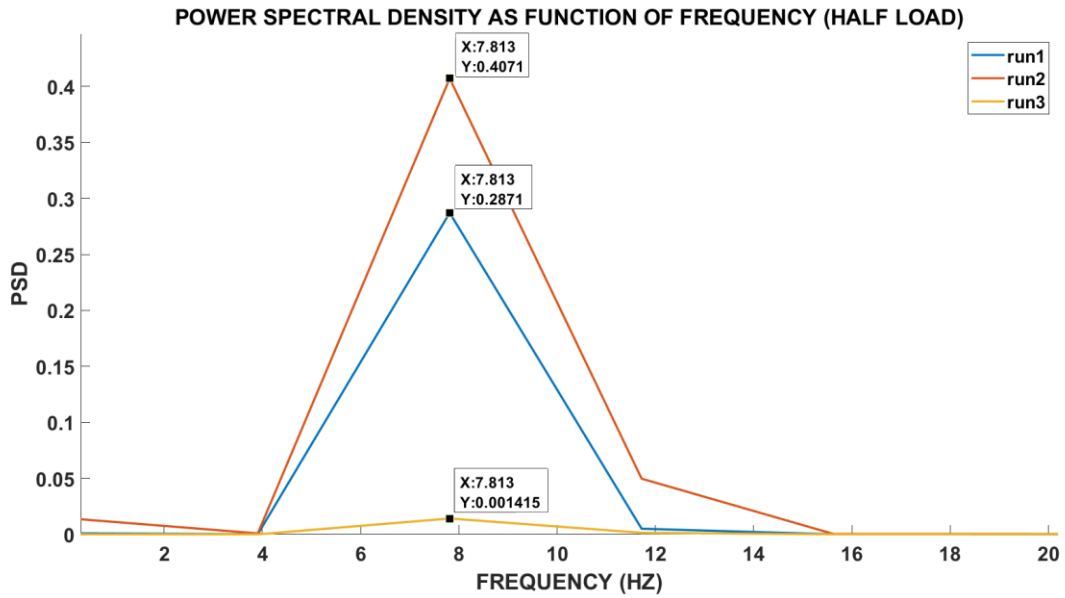

Figure 4.16: PSD as function of frequency for three repeated readings for half-load condition (FFT plot)

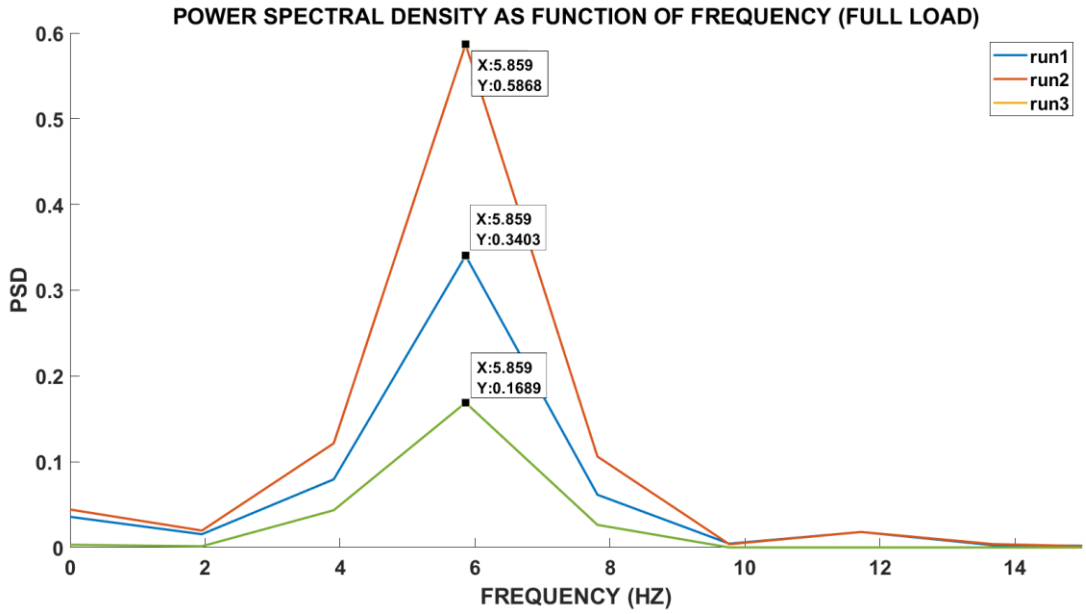

Figure 4.17: PSD as function of frequency for three repeated readings for full-load condition (FFT plot)

While amplitude gives us information about the strength of individual frequency components, PSD provides a broader view of how the signal's power is distributed across the frequency spectrum. Peaks observed in the PSD plot corresponds to specific frequencies at which the wing structure exhibits pronounced vibrational behavior and

this enables the precise determination of natural frequencies. The resulting plot of PSD (Power Spectral Density) as function frequency of first longitudinal mode resulted in a unique frequency for each loading conditions regardless of the number of repeated readings. This reinforced the reproducibility of the experiments. The natural frequency of the wing structure under no load condition corresponded to a value of 15.63 Hz, under half load condition corresponded to 7.81 Hz and under full load condition corresponded to 5.895 Hz. These are presented in Figure 4.15, 4.16 and 4.17 respectively. The observed decrease in natural frequency as the load on the wing structure increases suggests that the structure becomes less stiff or more flexible under heavier loads. Also loading a structure often means adding mass to it. The observed decrease aligns with expectations from the natural frequency equation $f = \frac{1}{2\pi}\sqrt{\frac{k}{m}}$, attributing it to increased mass and/or decreased stiffness under heavier loads.

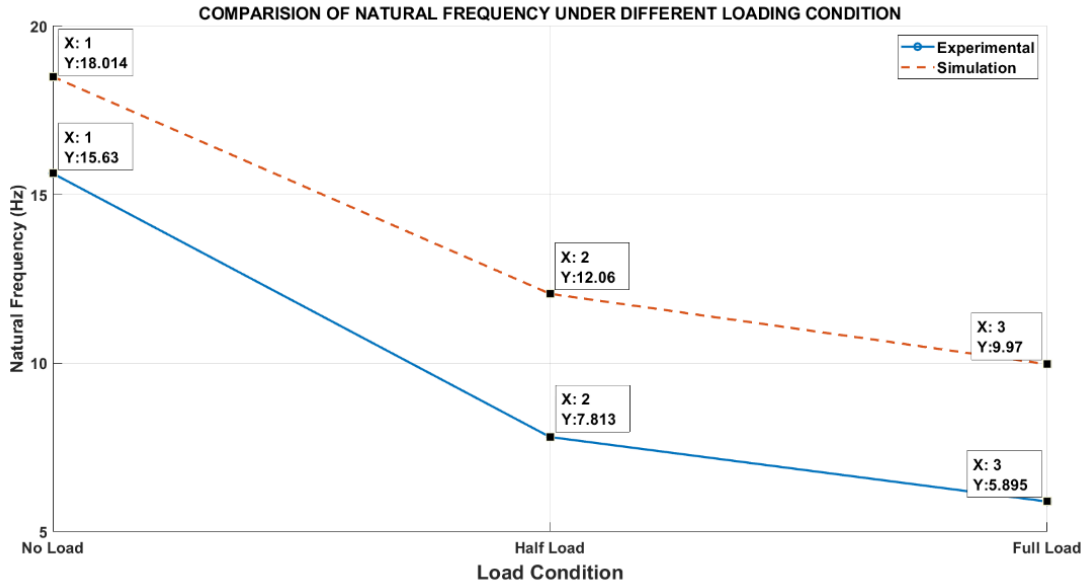

Figure 4.18: Plots comparing the trends of first modal frequencies from simulation and experiment under varying loading condition.

From the resulting plots presented in Figure 4.18, it can be concluded that the difference between the values of natural frequency between the modal analysis and experimental setup are not significant. The natural frequency variation trends of the simulated modal analysis and motion capture experiment are very similar. There is a 13.2 percent difference in the natural frequency values of the unloaded wing between the two methods. On the other hand, the difference between frequencies at half load and full load condition were 35 percent and 40.8 percent respectively. This indicated that the

discrepancy in results tends to increase as the load on the wing increases. The probable cause for this is assumed to be the non-linearity introduced by the weight added over the wing to simulate loads. This needs further investigation and has been recommended in future works.

The first mode of longitudinal vibration is considered to be the most significant mode of vibration for a cantilever wing model experiencing lift load. The range of frequency obtained for first mode of the designed wing was approximately in the domain of 5 Hz to 20 Hz. While the normal operating frequency domain of propulsion system is 150Hz to 400Hz. So, the most critical mode of vibration of the wing structure and the operating domain of propulsion system do not interfere with one another. The observed sharp decrease in natural frequency from no load to half load, followed by a more modest decrease from half load to full load, suggested potential nonlinear behavior in the wing structure's response to varying loading conditions. This trend suggests that as the wing experiences higher loads, the natural frequency range contracts to a lower value. Simultaneously, to accommodate elevated aerodynamic loads, the propulsion system must operate at a higher frequency. This observation not only signifies a reduced risk of resonance and fatigue loading but also highlights the safety and resilience of the wing under high load conditions. Modal frequencies play a crucial role in preventing resonance and dynamic instabilities, serving as a critical factor in ensuring the structural integrity and longevity of wings.

4.5.2 Wind Tunnel Test Result:

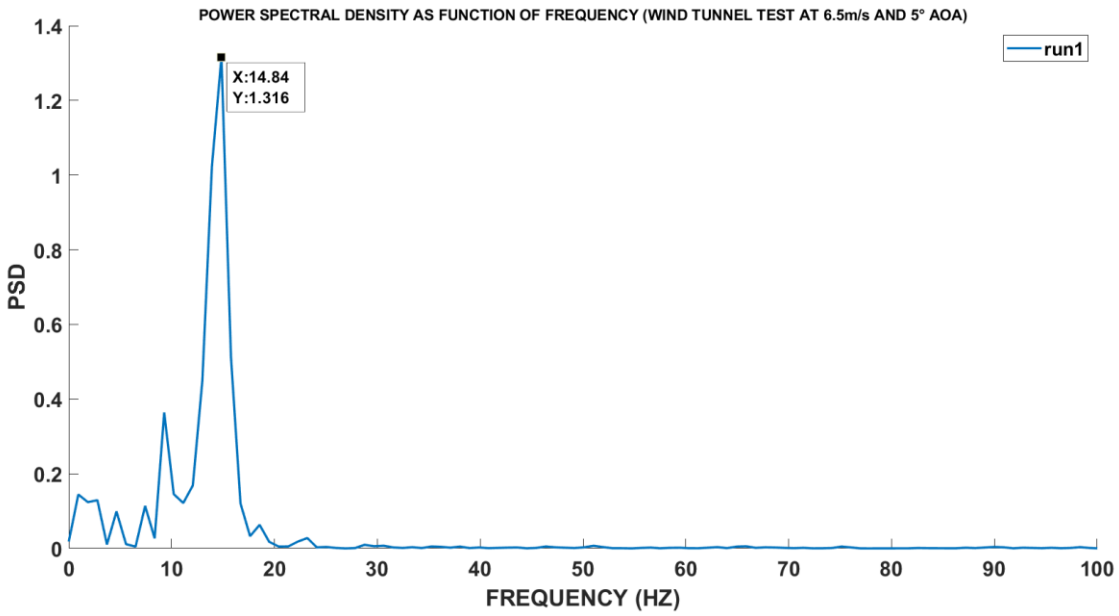

Figure 4.19: Power Spectral Density as Function of Frequency (at 6.5m/s and 5 ° AOA)

Image capture was employed to collect visual TIFF data from wind tunnel setup and analyzed in MATLAB and the resulting plot obtained by analyzing the data measurement provided a frequency of 14.84Hz as shown in Figure 4.19. This value of frequency obtained from wind tunnel test was close to the resulting frequency value of 15.63 Hz obtained at no load condition from experimental modal analysis.

4.5.3 Damping Ratio Analysis:

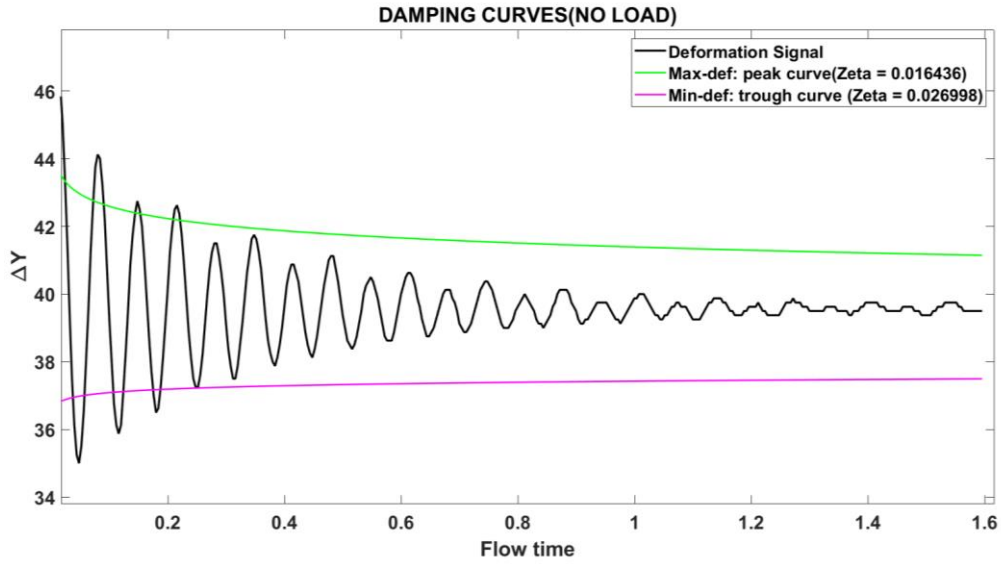

Figure 4.20: Damping curves for peaks and troughs of the deformation signal at no load condition.

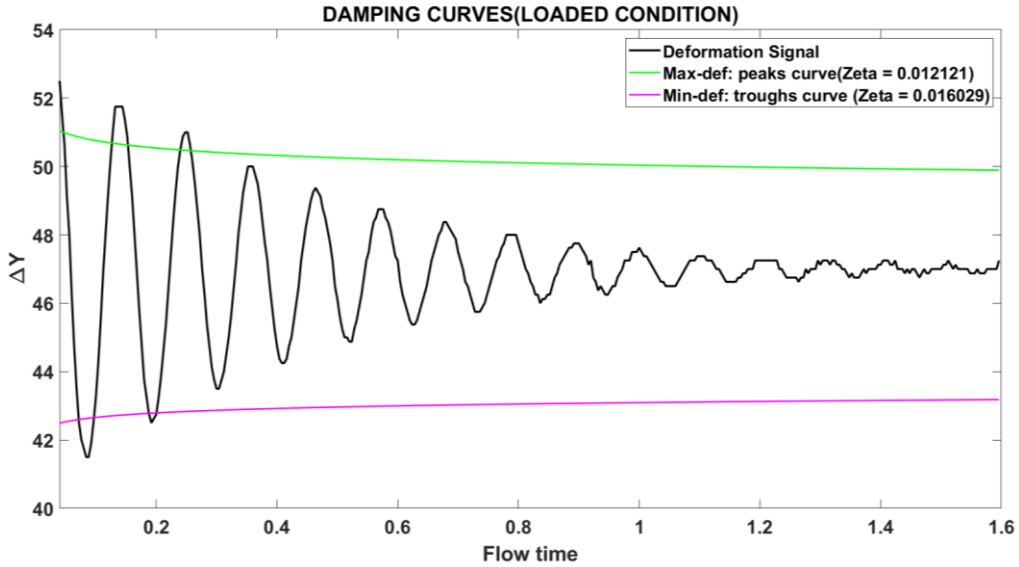

Figure 4.21: Damping curves for peaks and troughs of the deformation signal at loaded condition.

When moving from no load condition to 50 percent loading condition, the damping ratio of peaks decreased by 26.26 percent and that of trough decreased by 40.59 percent. The mean values of damping ratio for peaks and trough of the displacement curves are displayed in the legend section of Figure 4.20 and Figure 4.21. A lower damping ratio (closer to 0) indicates a more oscillatory and underdamped response. So, this shows

underdamped response of the wing is more pronounced at the loaded condition. On the other hand, a higher damping ratio (closer to 1) indicates that the system has faster and more critically damped responses, meaning that oscillations decay more quickly.

Lower damping ratio means the decrement in consecutive displacement value is lower. The results show that the wing appears to became less effective at dissipating energy and more prone to oscillations or vibrations when subjected to aerodynamic loading compared to no load condition. In practical terms, this change in damping behavior could have implications for the structural response. It affects the dynamic stability, resilience to external forces and the overall performance of the structure under different loading conditions.

CHAPTER FIVE: CONCLUSIONS AND RECOMMENDATIONS

5.1 Conclusion

i. This research used analytical and computational methods to establish design parameters for a UAV wing prototype. Problem framing and literature reviews guided the process, reinforced by iterative refinement of design through, scale model development, loading assessments and FEA analysis. This led to improvement in stiffness and tensile strength of the fabricated wing. Use of digital manufacturing technology and versatile materials like allowed for rapid iterative improvement in wing design, prototype development and testing.

ii. The initial plan to use a whiffletree rig for aerodynamic load proved impractical due to cost and complexity. After consultation, a shift to a simpler method employing wooden cradles and dead weights was implemented. This modification-maintained research integrity while reducing costs and logistical challenges.

iii. Modal analysis estimated natural frequencies under varying load conditions, followed by experimental testing employing a high-speed camera setup. Both the modal analysis and experimental testing showed a significant drop in natural frequency under varying loads, indicating potential nonlinear behavior.

iv. Damping ratio analysis showed decrease in value of damping ratio from no load condition to loaded condition indicating the wing was less capable to dissipate energy under aerodynamic loading. So, chances of flutter to occur is higher at higher loads.

The study concluded that increased loads contract the natural frequency range, reducing the risk of resonance and fatigue loading while highlighting the wing's safety and resilience. Based on the trend analysis plot depicted in Figure 4.18, the natural frequency variation trends of the simulated modal analysis and motion capture experiment are very similar. So, the comparison between modal analysis and experimental results affirmed research credibility, marking successful development and testing of a lightweight, strong, and durable UAV wing.

5.2 Recommendations

i. For the current research removal of air from the vacuum bag was done by a manually operated pump. Use of correct motor-powered vacuum pump will ensure enhancement and consistency of material properties in fabricated composite and further reduce wing weight.

ii. The discrepancy in results between simulation and motion tracking tended to increase as the load on the wing increased. Assuming non-linearity introduced by this weight is a probable cause can be a reasonable hypothesis. It can be a good foundation for further investigation to understand the intricacies of how the added load affects the natural frequencies.

iii. Analysis for higher modes of vibration can provide more insight into extent of relevance between experimental and simulation results. Further this will ascertain the identification of potential resonance phenomena in the higher modes and find critical points in the frequency domain.

iv. Permanent fixtures and rig structures like whiffletree, to test composite wings with larger aspect ratio, can be can be helpful in prompt conduction of such experiments.

v. Further analysis and correlation of results from the modal analysis setup and results from wind tunnel test under variable test conditions can help to verify the results of the experiments and provide insights on the discrepancies of aerodynamic loading representation if present.

REFERENCES

1. Mostakim, Z., Sajib, K. A., & Zabal, M. E. (2019). Vibration Analysis of Different Airfoils of Aircraft Wing. *Library of Islamic University of Technology (IUT).*

2. Oladele, I. O., Omotosho, T. F., and Adediran, A. A. (2020). Polymer-Based Composites: An Indispensable Material for Present and Future Applications. *International Journal of Polymer Science, 2020.*

3. Morimoto, Y. (2020). High-Speed Measurement of Shape and Vibration: Whole-Field Systems for Motion Capture and Vibration Modal Analysis by OPPA Method. *Sensors, 20*(15), 4263.

4. Aerospace Engineering Blog (2017). Aeroelasticity, composites and the Grumman X-29.Retrieved from https://aerospaceengineeringblog.com/aeroelasticity-composites-and-the-grumman-x-29/ on (2023, September 23).

5. Drang, A. (2014, April 12). Damped free vibrations. Retrieved from https://leancrew.com/all-this/2014/04/damped-free-vibrations/

6. Kelly, S. G. (2011). *Mechanical vibrations: Theory and applications*. Cengage Learning.

7. Grodzki, W., & Łukaszewicz, A. (2015). Design and manufacture of unmanned aerial vehicles (UAV) wing structure using composite materials. *Materialwissenschaft und Werkstofftechnik, 46.*

8. Budarapu, P. R., B., S. S. Y., & Natarajan, R. (2016). Design concepts of an aircraft wing: composite and morphing airfoil with auxetic structures. *Frontiers of Structural and Civil Engineering, 10*(4), 394-408.

9. Shiva, S., Pranjal, P., Kukal, R., Kumar, S., & Singh, G. (2020). Design and Fabrication of Wing of a High-Payload Aerial Vehicle. *International Journal of Mechanical and Production Engineering Research and Development, 10,* 551-562.

10. Bramesfeld, G., & Prinster, R. (2015). Design and testing of foam-inflated wings for small unmanned aerial vehicles. *Journal of Unmanned Vehicle Systems, 3*(4), 176-191.

11. Lamani, S., Dsouza, S., Saldanha, D. H., Dsouza, G., & Londhe, M. R. (2020). Analysis, fabrication, and testing of a sandwich composite for a UAV wing. *AIP Conference Proceedings, 2311.*

12. El Adawy, M., Abdelhalim, E. H., Mahmoud, M., Abo zeid, M. A., Mohamed, I. H., Othman, M. M., ... ElShabasy, Y. H. (2023). Design and fabrication of a fixed-wing Unmanned Aerial Vehicle (UAV). *Ain Shams Engineering Journal, 102094.*

13. Simsiriwong, J., & Sullivan, R. (2012). Experimental vibration analysis of a composite UAV wing. Mechanics of Advanced Materials and Structures, 19(1-3), 10.

14. Srividhya, S., Nehru, K., Rago, A. S., & Selvan, P. (2020). Vibrational analysis of an aircraft wing model using ANSYS Workbench. *International Journal of Engineering Development and Research*, 8(3), 44-49.

15. Pungoti, V., Prasad, B. S., Chandra Shekar, K., & Ramana Reddy, D. V. (2014). Design and analysis of A320 wing using E-Glass epoxy composite. *International Journal of Engineering Research & Technology (IJERT), 3*(11), 1385-1393.

16. Mabbrur, A. M., El Amien Noor Pamungkas, H., Syaifer, N., Fawwaz Nadzir, S., El Amien P, H. N., Sari Syaifer, N., & Hidayat, A. (2019). UAV Wing Structure with 3D Printed PLA Filament Wing Spar. *ResearchGate.*

17. Pandav, P. A., & Sawanti, D. A. (2017). Experimental evaluation and analysis of Glass Fiber Reinforced Composite under mechanical loading by using FEA software. *2017 International Conference on Recent Advances in Engineering and Technology (ICRAET).*

18. Sullivan, R., Hwang, Y., Rais-Rohani, M., & Lacy, T. (2014). Structural Analysis and Testing of an Ultralight Unmanned-Aerial-Vehicle Carbon-Composite Wing. *IEEE Transactions on Vehicular Technology, 63(1), 140-147.*

19. Kurnyta, A., Zielinski, W., Reymer, P., & Dragan, K. (2020). Numerical and Experimental UAV Structure Investigation by Pre-Flight Load Test. *Materials, 13(15).*

20. Jablonski, J. M. (2021). Light-Airplane Wing Structural Analysis and Material Selection. *M.S. thesis, Oregon State Univ., Corvallis, OR, USA*

21. Chandekar, C. G. S., Thatte, B. S., & Kelkar, A. D. (2010). On the Behavior of Fiberglass Epoxy Composites under Low Velocity Impact Loading. *Advances in Mechanical Engineering.*

22. Ferreira, J. F. M. A. (2018). Structural Analysis and Optimization of a UAV Wing. *Master's thesis, Instituto Superior Técnico, Unive. de Lisboa, Portugal.*

23. Sharba, M. J., Salman, S. D., Leman, Z., Sultan, M. T. H., Ishak, M. R., & Azmah Hanim, M. A. (2016). Effects of processing method, moisture content, and resin system on physical and mechanical properties of woven kenaf plant fiber composites. *BioResources, 11*(1), 1466-1476.

24. M. Utami, J. Ernest Sirait, B. Budhi Septyanto, A. Sudiarso, and I. N. Putra Apriyanto, "Laminar Composite Materials for Unmanned Aircraft Wings," *Defense and Security Studies*, vol. 3, pp. 106-112, 2022.

25. Abdurohman, K., Satrio, T., Muzayadah, N. L., & Teten. (2018). A comparison process between hand lay-up, vacuum infusion, and vacuum bagging method toward E-glass EW 185/Lycal composites. *Journal of Physics: Conference Series, 1130*.

26. Zhang, W., Liu, Y., & Qin, X. (2021). Computer vision tracking techniques applied to vibration analysis.

27. Simsiriwong, J., Rais-Rohani, M., Qatu, M., & Lacy Jr., T. (2009). Structural testing of an ultralight UAV composite wing and fuselage. *Scholars Junction.*

28. Wikipedia. (n.d.). Modal testing. Retrieved September 17, 2023, from https://en.wikipedia.org/wiki/Modal_testing.

29. gfai tech GmbH. (2023, January 11). Impact Hammer WaveHitMAX | gfai tech. Retrieved from https://www.gfaitech.com/products/structural-dynamics/impact-hammer-wavehit-max. [Accessed: July 21, 2023].

30. Śmieja, M., Mamala, J., Prażnowski, K., Ciepliński, T., & Szumilas, L. (2021). Motion magnification of vibration image in estimation of technical object condition-review.

31. Wood, A. (2023). Wing Structural Design. *AeroToolbox.* Retrieved from https://aerotoolbox.com/wing-structural-design/. [Accessed: March 21, 2023].

32. Sharma, S., Sharieff, U., Singh, A., & Tarnacha, R. S. (2021). Design and Fabrication of Fixed-Wing UAV for Commercial Monitoring. *International Research Journal of Engineering and Technology (IRJET)*, 2021.

APPENDIX A: Fabrication Processes

Wet layup of fiberglass with resin using a spreader

Weight measurement of resin mixture

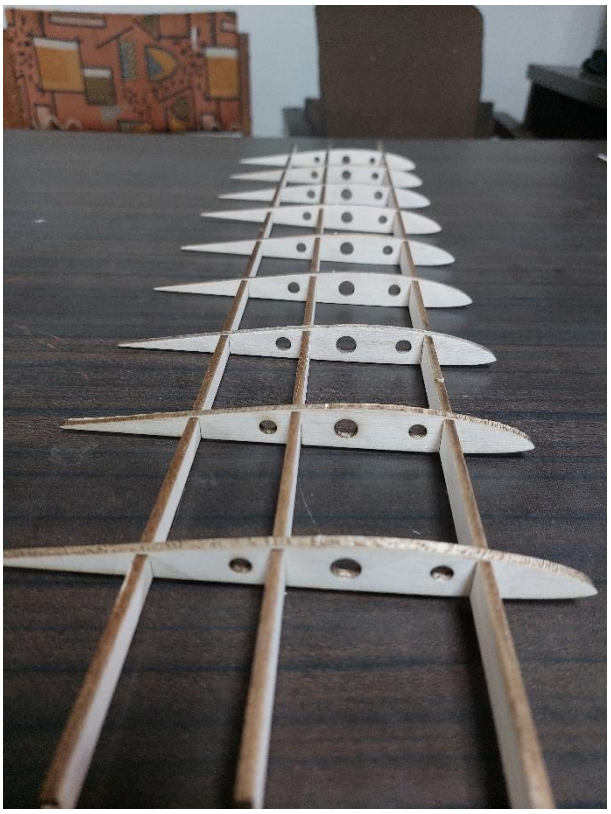

Assembly of 3.175mm thick balsa frame structure

Weight measurements of 3.175mm thick frame structure

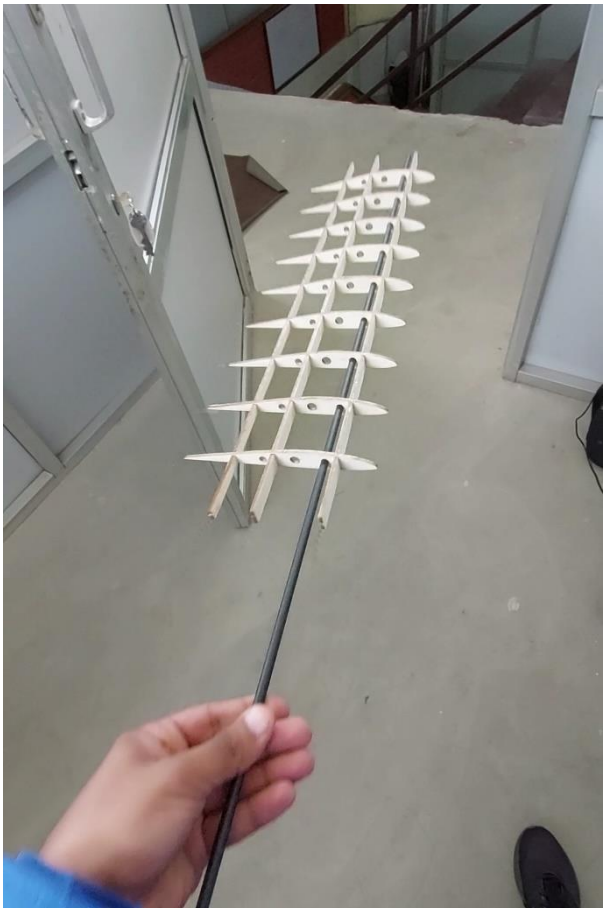

Image showcasing 3.175mm balsa frame structure

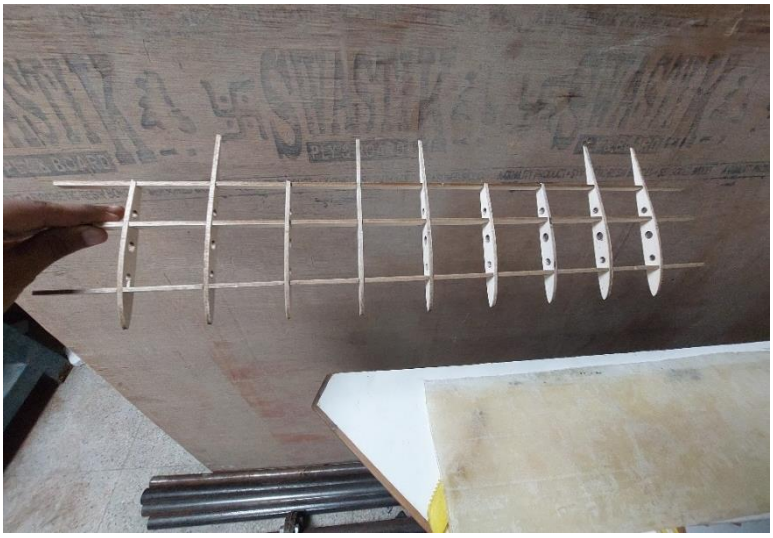

3.175mm thick balsa frame structures failing during assembly due to design flaws.

Removal of the foam core from the skin using hotwire

Assembling carbon fiber rod with balsa frame structure for improvised design

APPENDIX B: Experimental Setups

Overview of experimental data collection process

Wind velocity being measured

APPENDIX C: Software Results

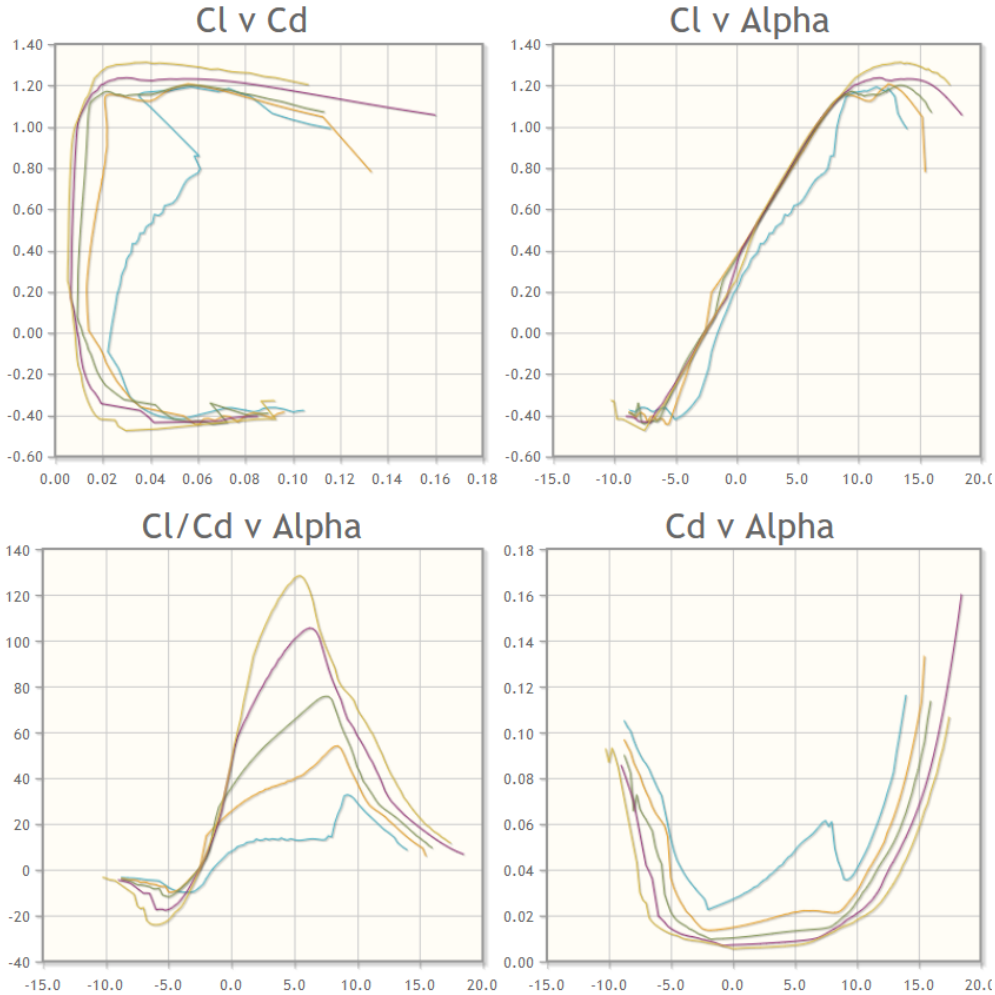

Graphical plots depicting the properties of Eppler 205 airfoil

Source: (Airfoil Tools, 2023)

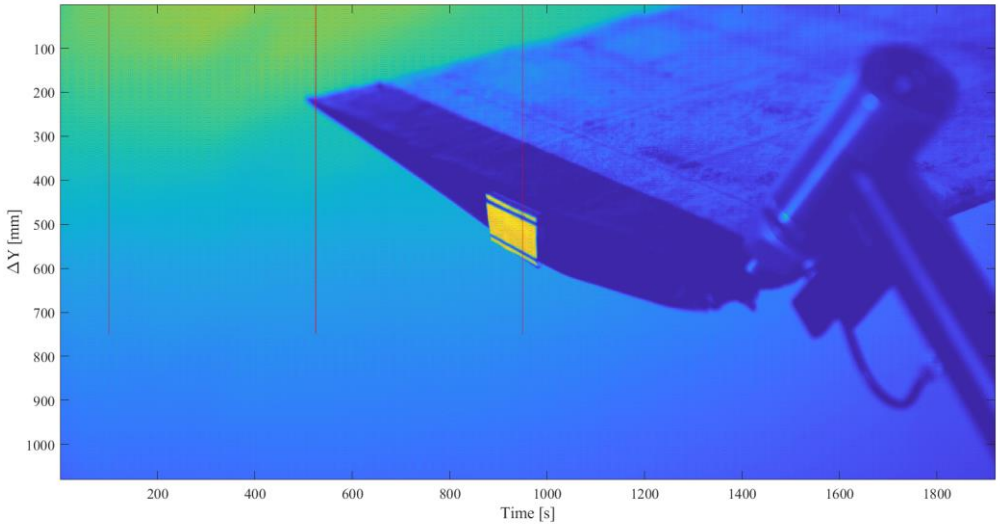

Image processing in MATLAB

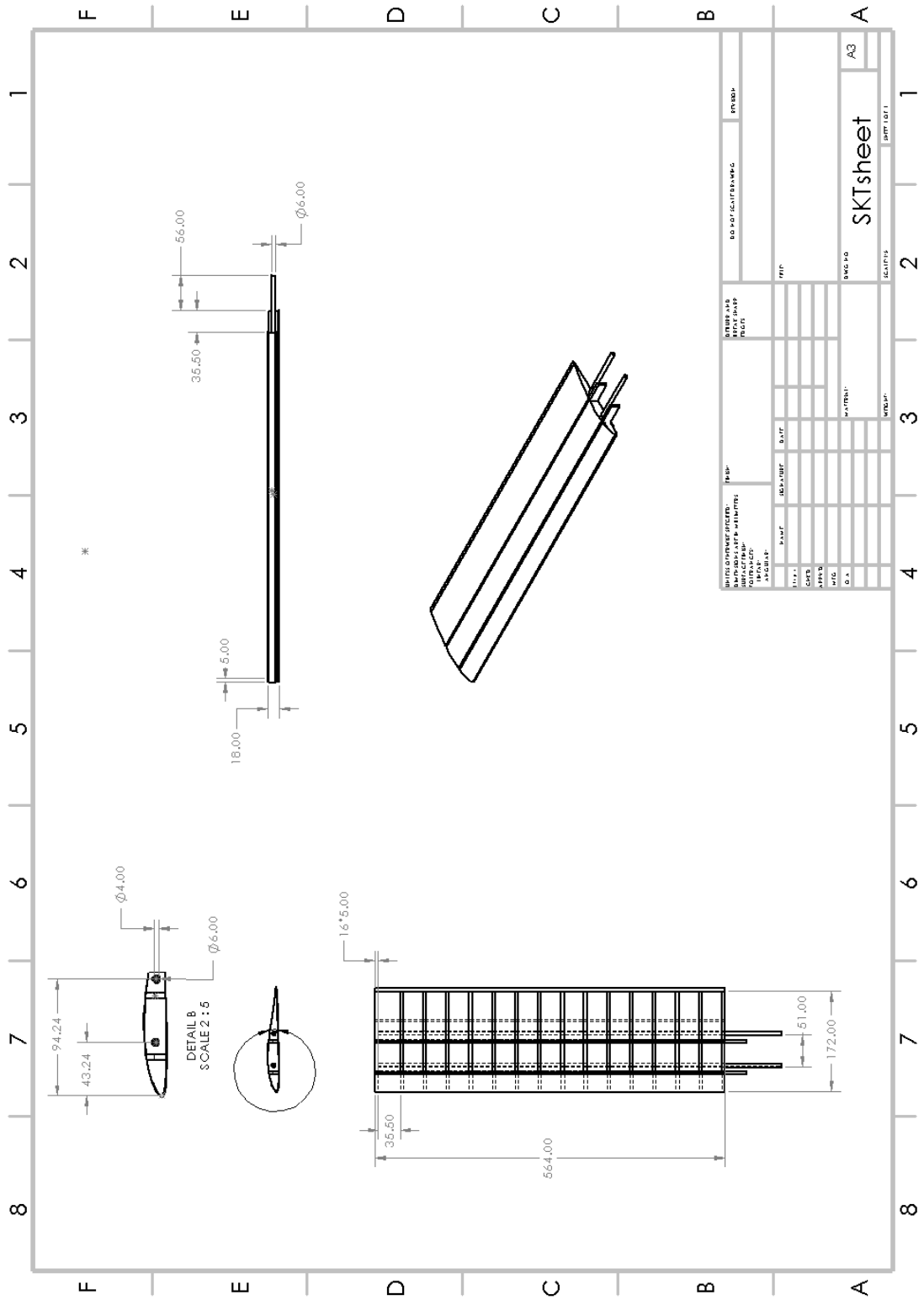

Detailed drawing views of the designed wing

Experimental Characterization and Aeroelastic Analysis of a Composite Wing

ORIGINALITY REPORT

12%
SIMILARITY INDEX

PRIMARY SOURCES

1	onlinelibrary.wiley.com Internet	215 words — 2%
2	www.ncbi.nlm.nih.gov Internet	144 words — 1%
3	www.ijedr.org Internet	111 words — 1%
4	scholarsjunction.msstate.edu Internet	91 words — 1%
5	doaj.org Internet	83 words — 1%
6	www.gfaitech.com Internet	77 words — 1%
7	www.ijert.org Internet	73 words — 1%
8	aerospaceengineeringblog.com Internet	65 words — 1%
9	www.ukessays.com Internet	65 words — 1%
10	www.researchgate.net Internet	

57 words — < 1%

11 journal.hep.com.cn
Internet
56 words — < 1%

12 Mohammed El Adawy, Elhassan H. Abdelhalim, Mohannad Mahmoud, Mohamed Ahmed Abo zeid et al. "Design and fabrication of a fixed-wing Unmanned Aerial Vehicle (UAV)", Ain Shams Engineering Journal, 2023
Crossref
43 words — < 1%

13 R. Warsi Sullivan, Y. Hwang, M. Rais-Rohani, T. Lacy. "Structural Analysis and Testing of an Ultralight Unmanned-Aerial-Vehicle Carbon-Composite Wing", Journal of Aircraft, 2009
Crossref
42 words — < 1%

14 slidelegend.com
Internet
41 words — < 1%

15 ir.library.oregonstate.edu
Internet
32 words — < 1%

16 J. Simsiriwong, R. Warsi Sullivan. "Experimental Vibration Analysis of a Composite UAV Wing", Mechanics of Advanced Materials and Structures, 2012
Crossref
29 words — < 1%

17 archive.org
Internet
26 words — < 1%

18 "Research Developments in Sustainable Aviation", Springer Science and Business Media LLC, 2023
Crossref
23 words — < 1%

19 Gautam S. Chandekar. "On the Behavior of Fiberglass Epoxy Composites under Low Velocity
23 words — < 1%

Impact Loading", Advances in Mechanical Engineering, 2010
Crossref

20 Priyadarsini Morampudi, Kiran Kumar Namala, Yeshwanth Kumar Gajjela, Majjiga Barath, Ganaparthy Prudhvi. "Review on glass fiber reinforced polymer composites", Materials Today: Proceedings, 2021 — 22 words — < 1%
Crossref

21 Tondji Chendjou, Yvan Wilfried. "Morphing Wing: Experimental Boundary Layer Transition Determination and Wing Vibrations Measurements and Analysis.", Ecole de Technologie Superieure (Canada), 2017 — 21 words — < 1%
ProQuest

22 oaji.net — 18 words — < 1%
Internet

23 Götz Bramesfeld, Ryan Prinster. "Design and testing of foam-inflated wings for small unmanned aerial vehicles", Journal of Unmanned Vehicle Systems, 2015 — 17 words — < 1%
Crossref

24 Natsuki Tsushima, Kenichi Saitoh, Kazuyuki Nakakita. "Structural and aeroelastic characteristics of wing model for transonic flutter wind tunnel test fabricated by additive manufacturing with AlSi10Mg alloys", Aerospace Science and Technology, 2023 — 14 words — < 1%
Crossref

25 core.ac.uk — 14 words — < 1%
Internet

26 W. Grodzki, A. Łukaszewicz. "Design and manufacture of umanned aerial vehicles (UAV) — 13 words — < 1%

wing structure using composite materials", Materialwissenschaft und Werkstofftechnik, 2015
Crossref

27 www.igi-global.com
Internet
13 words — < 1%

28 www.mdpi.com
Internet
12 words — < 1%

29 Haley, Ste. "Design Optimization and Verification of a Horizontal Stabilizer for the SeaStryder600 Wing-In-Ground-Effect (WIG) Aircraft", Proquest, 2014.
ProQuest
10 words — < 1%

30 Hummer, Christopher J.. "Computational Study of a Plate Mounted Finite Cylinder: Aspect Ratio and Boundary Layer Thickness Effects.", Proquest, 2014.
ProQuest
9 words — < 1%

31 "Sensors and Instrumentation, Aircraft/Aerospace, Energy Harvesting & Dynamic Environments Testing, Volume 7", Springer Science and Business Media LLC, 2022
Crossref
8 words — < 1%

32 vdocuments.mx
Internet
8 words — < 1%

33 www.ijera.com
Internet
8 words — < 1%

34 P. R. Budarapu, Sudhir Sastry Y B, R. Natarajan. "Design concepts of an aircraft wing: composite and morphing airfoil with auxetic structures", Frontiers of Structural and Civil Engineering, 2016
Crossref
6 words — < 1%

35 Shivaji Lamani, Stanvil Dsouza, Dane Hubert Saldanha, Granvil Dsouza, Madhurima R. Londhe. "Analysis, fabrication and testing of a sandwich composite for an UAV wing", AIP Publishing, 2020

6 words — < 1%

Crossref

EXCLUDE QUOTES	ON	EXCLUDE SOURCES	< 6 WORDS
EXCLUDE BIBLIOGRAPHY	ON	EXCLUDE MATCHES	OFF